Analyst

ROYAL SOCIETY OF CHEMISTRY

MINIREVIEW

View Article Online
View Journal | View Issue

Cite this: *Analyst*, 2025, **150**, 2469

Recent advances in biosensors based on the electrochemical properties of MXenes

Luming Pan,†[a] Dongtao Zhou†[b] and Yuzhen Wang *[a]

Biosensors have rapidly gained popularity and made significant progress in their applications in recent years, and a key strategy for the development of advanced biosensors is the utilization of novel structures with remarkable properties. The emergence of novel nanostructures will significantly improve the performance of sensors and create a new frontier for highly sensitive analysis. MXenes, as an emerging two-dimensional nanomaterial with a unique layered structure and electrochemical properties, have become an ideal material for developing high-sensitivity, high-stability, and multifunctional biosensors. In this review, we systematically summarized the synthesis and modification methods for MXenes and their current applications in biosensing, including electrochemical sensing, optical sensing, and wearable and portable sensing. Furthermore, this review offers potential solutions to address the challenges posed by MXenes in biosensor applications, specifically those related to material stability and biocompatibility. This review is believed to provide insights into the development of MXenes for biosensing, paving the way for their future translational medical applications.

Received 28th February 2025,
Accepted 26th April 2025

DOI: 10.1039/d5an00235d

rsc.li/analyst

1. Introduction

Biosensors are usually characterized by high selectivity, high sensitivity, and real-time monitoring, which are widely used in clinical diagnostics,[1] environmental monitoring,[2] food safety detection,[3] and personal health tracking.[4] For example, enzyme electrode-based blood glucose sensors have been widely used to monitor blood glucose levels in diabetic patients;[5] metal nanoparticle-based sensors have also been developed for water quality testing, enabling the efficient detection of heavy metal ions like lead, mercury, and other contaminants; antibody-based immunosensors could be used to detect harmful pathogens in food, such as salmonella.[6] Several materials have been applied to biosensors, such as metal nanoparticles,[7] carbon nanotubes,[8] and graphene.[9] These materials offer distinct performance characteristics, making them suitable for different types of biosensors. However, these biosensors still encounter several challenges in practical applications. One major issue is their limited sensitivity, particularly when detecting complex biological samples. This is often caused by interfering substances that reduce the signal-to-noise ratio, ultimately compromising the sensor's performance. Other issues include poor selectivity, with many sensors being easily affected by contaminants, and vulnerability to environmental factors like temperature and humidity, which can degrade sensor accuracy. Additionally, the high cost of preparation and difficulty in mass production remain significant barriers.

MXenes, a family of two-dimensional (2D) transition metal carbides, nitrides, or carbonitrides, were initially synthesized and characterized by the research group led by Prof. Yury Gogotsi in 2011.[10,11] The synthesis of MXenes was primarily accomplished through selective etching, which involves removing the A-layer from the MAX phase using an acidic solution containing fluorine (*e.g.*, HF and LiF + HCl), and MXene lamellae with a two-dimensional layered structure are thus formed. MXene flakes are then obtained through ultrasonic dispersion and liquid-phase exfoliation. Due to their two-dimensional nature, similar to graphene, the flakes are held together by weak van der Waals forces, making them prone to exfoliation and dispersion. During the synthesis process, the surface of MXenes was introduced with hydroxyl (–OH), fluorine (–F), and oxide (=O) groups. These groups are integral to their structure and impart unique properties to the MXene nanosheets. As a result, MXenes are considered a promising candidate for use as a carrier in biosensing,[12] environmental protection,[13] and signal transmission[14] applications. Moreover, MXenes exhibit several key features that make them a strong candidate for biosensor applications. Their high electrical conductivity, driven by the unique layered structure and electronic properties of transition metals, enables efficient

[a]*Key Laboratory of Flexible Electronics (KLOFE), Institute of Advanced Materials (IAM) & School of Flexible Electronics (Future Technologies), Nanjing Tech University, Nanjing 211816, China. E-mail: iamyzwang@njtech.edu.cn*
[b]*State Key Laboratory of Analytical Chemistry for Life Science, College of Engineering and Applied Sciences, Nanjing University, Nanjing, 210023, China*
†These authors contributed equally to this work.

signal transmission.[15] These materials also offer large specific surface areas, which provide abundant active sites for effective interaction with target molecules.[16] Additionally, MXene surfaces could be easily modified with functional groups (*e.g.*, –OH, –F, –O, *etc.*), improving their selectivity, stability, and biocompatibility, which enhance their performance in biosensors.[17] Furthermore, as two-dimensional materials, MXenes combine exceptional mechanical strength with a degree of flexibility, making them ideal for use in wearable or flexible sensors.[18] Finally, compared to other materials, MXenes demonstrate superior biocompatibility, minimizing the risk of toxicity when used in biological systems or *in vitro* applications.[19]

This review provides a systematic overview of the advantages of MXenes in biosensor development, highlighting innovations in synthesis strategies, sensing mechanisms, and practical applications. Firstly, we discuss the basic properties of MXene materials, synthetic methods, and surface modification functionalization approaches. Secondly, we explore the advantages of MXene materials in the field of biosensors and the use of MXenes' excellent electrochemical properties as a biosensing material in electrochemical sensors, optical biosensors, and wearable portable biosensors. Along with a detailed examination of MXene materials, we also discuss the challenges that MXenes face in practical biosensor applications. We anticipate that this review will offer fresh perspectives and guidance for advancing the development of MXene nanocomposite-based biosensors that are efficient, highly selective, and sensitive.

2. Synthesis and surface modification of MXenes

2.1. Synthesis of MXenes

The MAX phase is a unique family of layered composite materials characterized by the general formula $M_{n+1}AX_n$ (Fig. 1), where M stands for a transition metal (such as Ti, Nb, Ta, Mo, or Cr), A is usually an element from groups IIIA or IVA (like Al, Si, Ga, or Sn), and X represents either carbon (C) or nitrogen (N). The structure of MAX phases consists of alternating M and X layers, with A layers positioned between them, forming a three-dimensional lamellar crystal structure. For example, in the widely studied MAX phase Ti_3AlC_2, Ti serves as the transition metal, Al as the A element, and C as the X component. Since the MAX phase material has a layered structure with weak van der Waals force interactions between the layers, it is somewhat exfoliative and easy to remove the A-layer by chemical etching, which provides the conditions for the synthesis of MXenes. MAX phase materials have excellent properties of both metals and ceramics. They have good electrical and thermal conductivity and plasticity and, at the same time, exhibit the high hardness, high temperature, and corrosion resistance of ceramics. MAX phase materials demonstrate excellent stability at elevated temperatures and in corrosive environments, as well as remarkable mechanical strength and resilience. Following the etching process, the structure of MXenes becomes increasingly lamellar, resulting in the formation of a two-dimensional layered structure comprising transition metals (M) and carbon or nitrogen (X). For example, $Ti_3C_2T_x$ MXenes are obtained from a Ti_3AlC_2 MAX phase material by a selective etching process involving the use of hydrofluoric acid (HF) to remove the Al layer. Graphene is a two-dimensional material that has been used in the field of biosensors,[20] which include electrochemical sensing,[21] optical sensing,[22] and biomolecular recognition.[23] Nevertheless, the advancement of graphene has encountered significant obstacles, primarily due to its high production costs, considerable variability in properties across different graphene samples, and the challenge of scaling up production. Given that MXenes have a structure that is highly similar to that of graphene and that their performance in electrochemical applications exceeds that of graphene. It can therefore be concluded that biosensors based on the electrochemical performance advantages of MXenes outperform those based on graphene.

At present, the most prevalent method for synthesizing MXenes is wet chemical etching. The most commonly used etching agents are hydrofluoric acid (Fig. 2A),[24] chloride solutions (*e.g.*, $FeCl_3$ and $CuCl_2$),[25,26] and mixed solutions of hydrogen chloride (HCl) and lithium fluoride (LiF).[27] For example, Wang *et al.* investigated the impact of HF etching on the microstructure of $Ti_3C_2T_x$ and their capacitive properties. They conducted the etching process on a Ti_3AlC_2 MAX phase material mixed with a 40% aqueous HF solution under stirring conditions for 0.1 to 17 days. The reaction is typically conducted at room temperature, within the range of 20 to 40 °C. The use of HF results in the removal of the A layer, comprising the element Al, leaving the transition metal layer (Ti) and the carbon layer (C) intact.[28] The reaction formula is presented below:

$$TiAlC_2 + 3HF \rightarrow Ti_3C_2 + 3H_2 + AlF_3 \quad (1)$$

The mixed products resulting from the etching process were subjected to a series of purification steps, including water washing and centrifugation, to remove excess fluoride. The dispersion was then washed until it reached a neutral pH value, thereby obtaining an MXene dispersion with a specified concentration. By controlling the etching time of the MAX phase material, observing the changes in internal stress and layer cracks in Ti_3AlC_2, and comparing the maximum specific capacitance of MXene materials obtained with different etching times to determine the optimal etching time. This serves as a valuable framework for synthesizing MXene materials with outstanding electrochemical performance.

Fluoride-based etching methods are widely applied due to their simplicity and versatility in synthesizing a broad range of MXenes. However, these synthetic methods pose challenges for scalability, hindering their practical applications. Therefore, Ghidiu *et al.* used a LiF and HCl mixed solution[29] instead of HF etching and synthesized MXenes with plasticity and high volumetric capacitance with potential for various applications with the following reaction formula:

$$Ti_3AlC_2 + 3LiF + 3HCl \rightarrow Ti_3C_2 + 3LiCl + 3H_2 \quad (2)$$

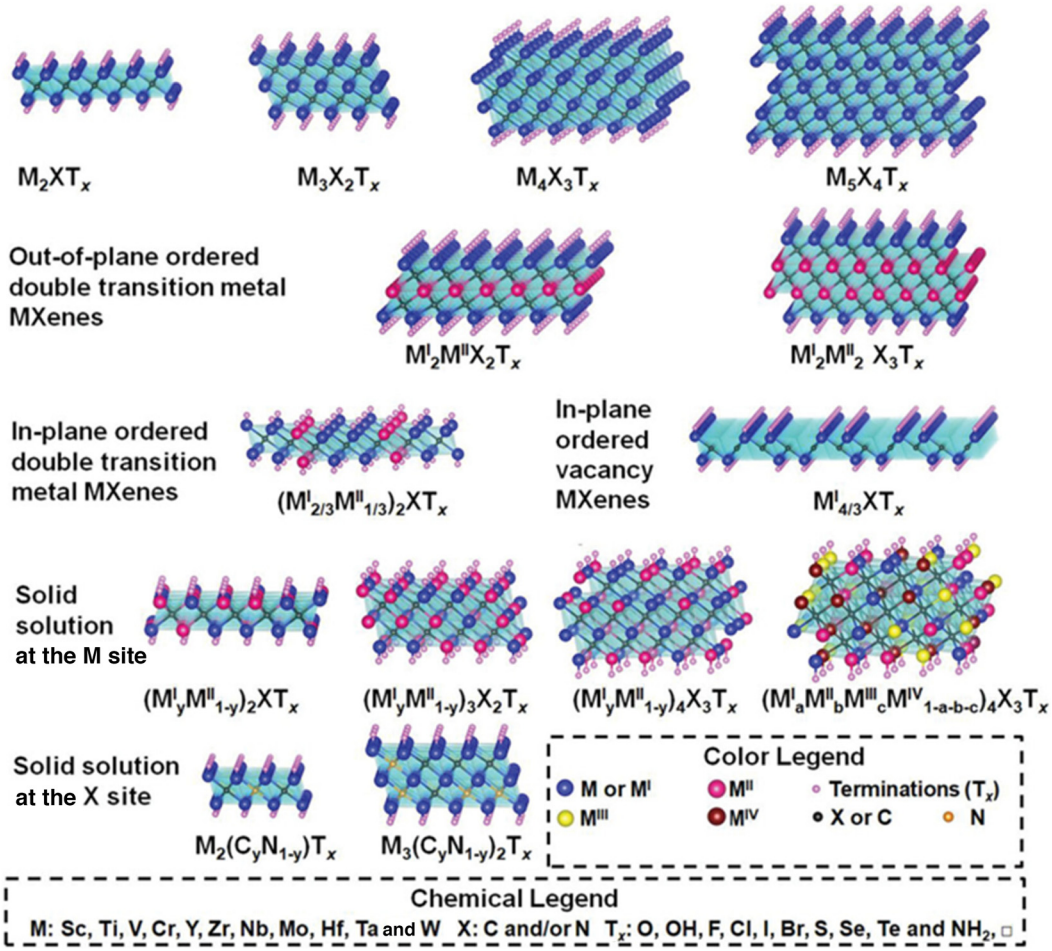

Fig. 1 Typical MXene structures and compositions. Reproduced from ref. 10 with permission from WILEY, copyright 2021.

Interestingly, similar to HF etching, LIF/HCl etching leads to the formation of accordion-like multilayered MXenes, which can be employed directly in a multitude of applications, including supercapacitors, desalination, and sensors.[30] The LiF + HCl etching method is capable of circumventing the utilization of the potent acid HF while concurrently reducing environmental contamination; however, it necessitates a protracted reaction time. As shown in Fig. 2B–F, Tian *et al.* used LiF/HCl to prepare an MXene material and employed a simple vacuum filtration method by using polystyrene (PS) spheres with different sizes (50–500 nm) and weight proportions (PS/MXene = 1/1, 1/3, and 1/6) as sacrificial templates to fabricate self-supporting carbon@MXene electrodes with three-dimensional (3D) mesoporous structures. The self-supporting electrodes can be used to monitor biological signals from fingers, wrists, arms and throat.[31]

Molten salt etching employs molten salts as an etchant to remove aluminum, primarily by reacting with the aluminum layer in the MAX phase. Molten salts typically comprise chlorides, fluorides, or chlorofluoride mixtures. Arole *et al.* employed SnF_2 to etch Nb_2CT_x sheets utilizing Nb_2AlC as a substrate under an argon atmosphere at 750 °C for 6–36 hours. The reaction produced 76% Nb_2CT_x clay, which was then subjected to hydroxyl modification.[32] Urbankowski *et al.* used fluoride salts in the molten state to etch Al of Ti_4AlN_3 powder species under an argon atmosphere at 550 degree Celsius. Both few-layer and single-layer $Ti_4N_3T_x$ nanosheets were obtained by delaminating the prepared MXene.[27,33]

Gas-phase selective etching represents a novel approach to the preparation of MXenes, whereby the A layer is selectively removed from the MAX phase through a gas-phase reaction, while the transition metal and carbon (or nitrogen) layers are retained. This method addresses some of the limitations of conventional wet etching (*e.g.*, HF solution etching), such as environmental contamination and liquid handling issues. Guo *et al.* developed a minute-scale production method. The high chemical activity of metal chloride vapor on the interlayer A-metal layer of the MAX phase makes it an ideal platform for the production of MXenes (Ti_2CCl_x) by selective etching of the MAX phase material (Ti_2AlC) under metal chloride ($ZnCl_2$) vapor.[34] This approach has been used effectively for electrocatalysis by Zhu *et al.* As shown in Fig. 3, MXenes (Ti_2CCl_x) were synthesized by etching the MAX phase material using halogen gases (such as Cl_2, Br_2, and I_2) or hydrogen halide gases (like HCl, HBr, and HI), leading to the formation of MXenes.[35]

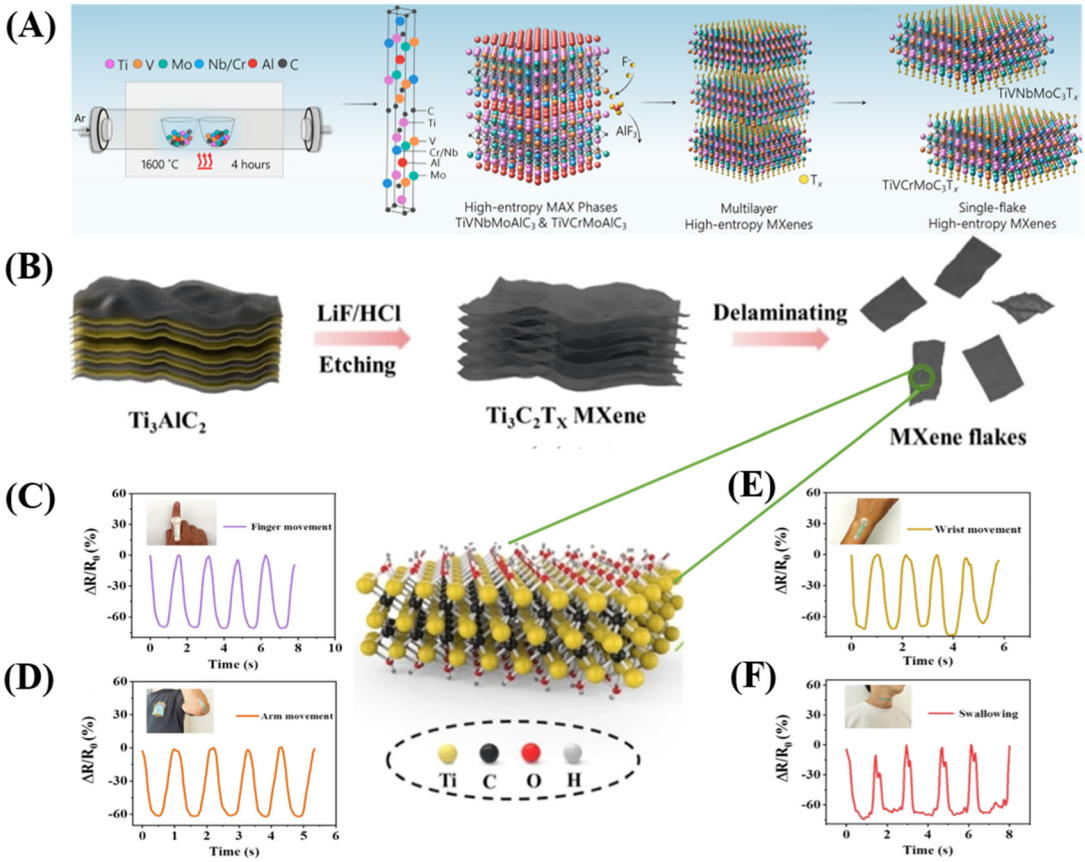

Fig. 2 (A) Schematic for the synthesis of high-entropy MAX and MXenes (etched by aqueous hydrofluoric acid). Reproduced from ref. 24 with permission from American Chemical Society, copyright 2021. (B–F) Preparation of MXenes using LiF/HCl and applications in sensing. Reproduced from ref. 31 with permission from American Chemical Society, copyright 2021.

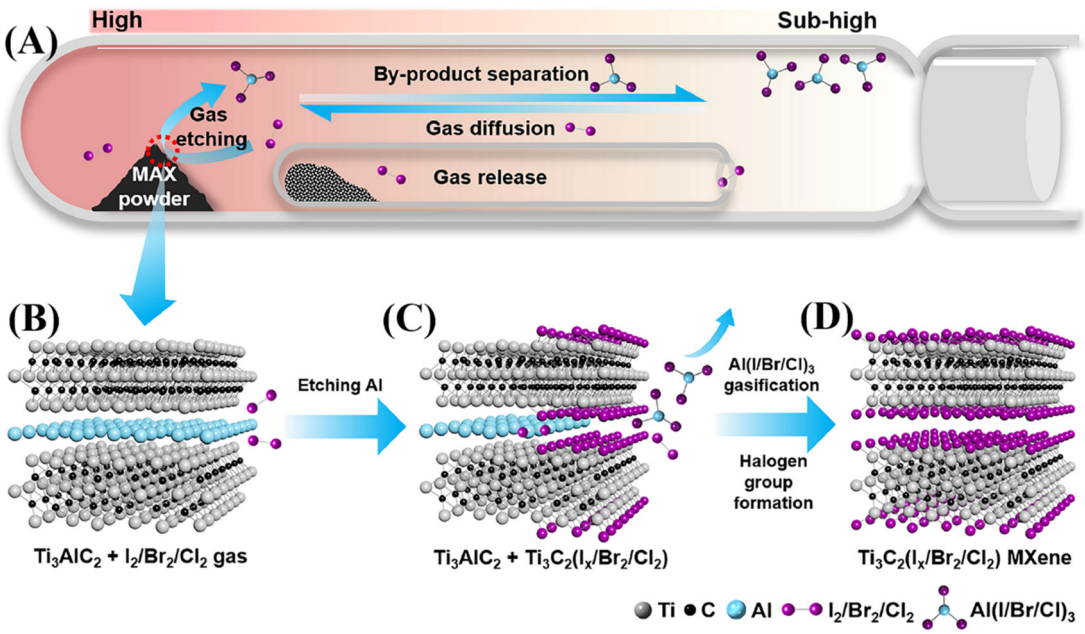

Fig. 3 (A–D) Schematic of gas etching to prepare MXenes. Reproduced from ref. 35 with permission from ELSEVIER, copyright 2024.

Subsequently, a suitable etching temperature (873 K) was determined by regulating the etching temperature to regulate the etching of elemental Ti, which significantly reduced the occurrence of Ti atoms. Furthermore, it has been demonstrated that the use of I_2 for etching MXenes results in the formation of additional functional groups.

The preparation of MXenes by electrochemical etching represents a novel method that ensures the absence of fluoride ions on the MXene surface throughout the etching process. Consequently, the surface of the synthesized MXene is comprised solely of hydroxyl (–OH) and chlorine (–Cl) groups.[36] Liu *et al.* synthesized Ti_2AlC MAX with tunable one-dimensional and two-dimensional morphologies by annealing at 950 °C in the first step, using CNT and rGO as carbon sources (Fig. 4A). In this process, the MAX phase served as the working electrode, a molten salt crucible acted as the counter electrode, and a glass-carbon rod was employed as the quasi-reference electrode. The one-pot electrochemical etching step, conducted *in situ* at 500 °C, successfully transformed Ti_2AlC MAX into Ti_2CT_x MXene.[37] Chan *et al.* used HBF_4 as the electrolyte and Pt wire as the cathode, with the anodic polarisation of the MAX phase triggering the dissolution of aluminum (Fig. 4B–D). The time and temperature required for etching in HBF_4 species were subsequently reduced by varying the applied voltage, and the release of HF during etching was diminished. The electrochemical etching of HBF_4 was observed to be a gentler, faster, and safer process than conventional chemical methods utilizing HF-based etchants, with yields reaching as high as 85%.[38] The synthesis of MXenes can be achieved through a number of different methods, each with its own distinctive advantages and limitations. It is possible that more efficient, environmentally friendly, and low-cost synthesis methods may be proposed in the future as a result of further research and technological advancement. In conclusion, the preparation of two-dimensional MXene sheets with high electrochemical properties represents a crucial step in their potential application in biosensors. Table 1 summarizes the basic methods for synthesizing MXenes.

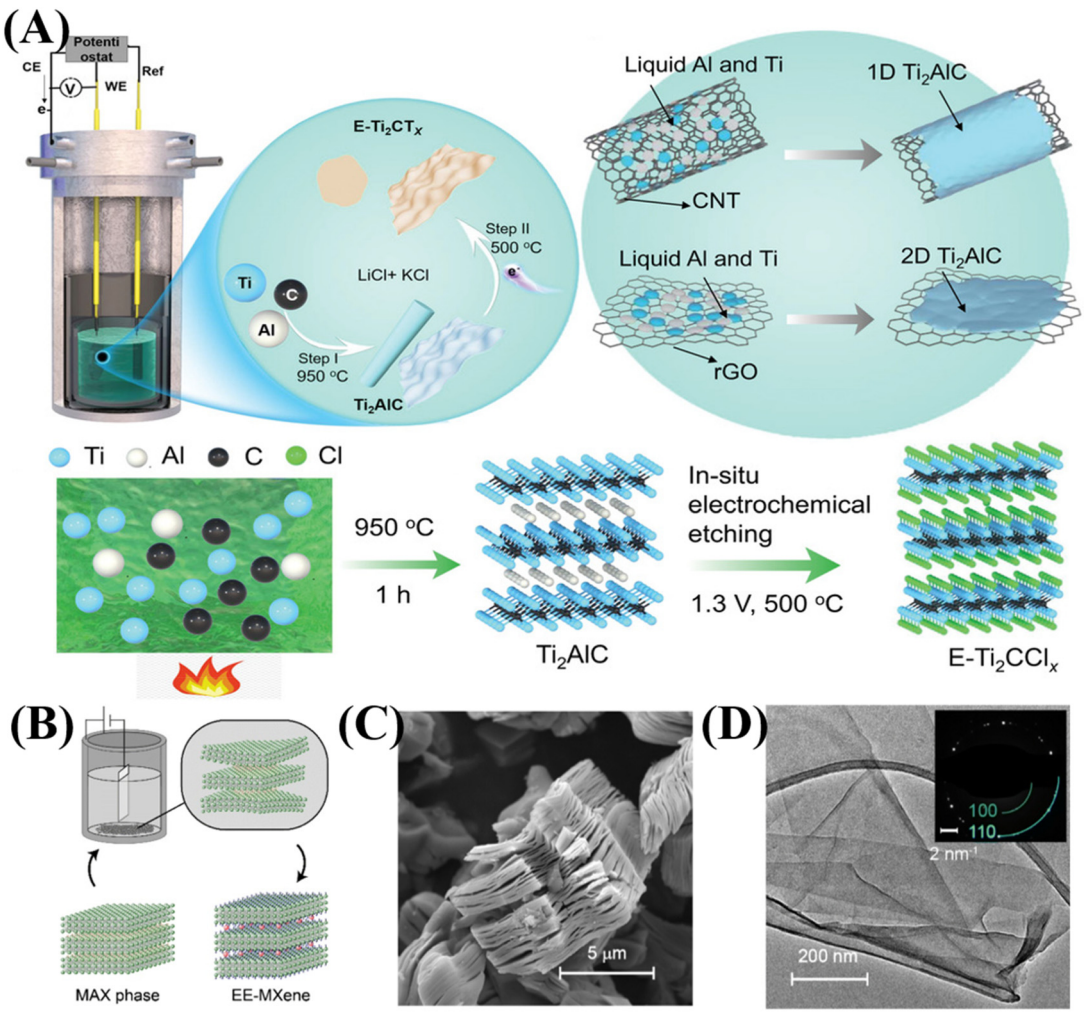

Fig. 4 (A) Schematic illustration of the fabrication process of Ti_2AlC and E-Ti_2CT_x. Reproduced from ref. 37 with permission from WILEY, copyright 2023. (B) Schematic illustration of the setup to etch EE-Ti_2C_3. (C) SEM image of EE-Ti_3C_2 multilayer powder. (D) TEM image of a delaminated EE-Ti_3C_2 flake. Reproduced from ref. 38 with permission from the Royal Society of Chemistry, copyright 2024.

Table 1 Methods for synthesizing MXenes

Method	Etchant	Advantages	Disadvantages	Ref.
Hydrofluoric acid (HF) etching	HF	Simple process, fast etching rate, high yield, and rich surface functional groups	Toxic and uneven functional groups	28
MILD (*in situ* generation of HF)	HCl + LiF	Safety, uniform surface functional groups, and high stripping efficiency	Long reaction time, high cost, and restricted types	27 and 29
Molten salt etching	$ZnCl_2$/KCl/LiF (molten salt system)	A wide range of etching possibilities, fluorine-free, and productive	High temperatures, complex process, and high costs	32 and 33
Electrochemical etching	Weakly acidic electrolyte (*e.g.* H_2SO_4)	Tender conditions and a controllable number of layers	High cost and complexity of requirements	37 and 38
Gas-phase selective etching	Cl_2, I_2, *etc.*	Product high conductivity	High temperature conditions	35
	$TiCl_4/CH_4$, *etc.*	Large area preparation and excellent compatibility	Equipment complexity, high cost, and poor controllability	

2.2. Surface modification of MXenes

Surface modification and functionalization of MXenes are key factors to enhance their sensitivity and selectivity in biosensors. By chemically modifying the surface of MXenes, it is possible to effectively regulate their surface properties, increase their biocompatibility, and improve their sensitivity and selectivity, thus promoting their wide application in biosensors. The improvement in biosensor performance through the surface modification and functionalization of MXenes is primarily seen in the following ways: firstly, surface modifications of MXenes can increase their affinity for target molecules, thereby enhancing the biosensor's response range and speed. Divya *et al.* modified MXene materials with gold nanoparticle-modified biomimetic bilayer lipid membranes (AuNP@BLM), and the synergistic combination of MXenes and AuNP@BLM proved to be effective in increasing the detection signal by several fold.[39] Wang *et al.* developed TDN-modified MXenes as innovative probes for gliotoxin sensing (Fig. 5A). MXene nanosheets provide a large surface for TDN adsorption and signal transduction, with the titanium on their surface facilitating easy assembly of TDNs without costly or complex

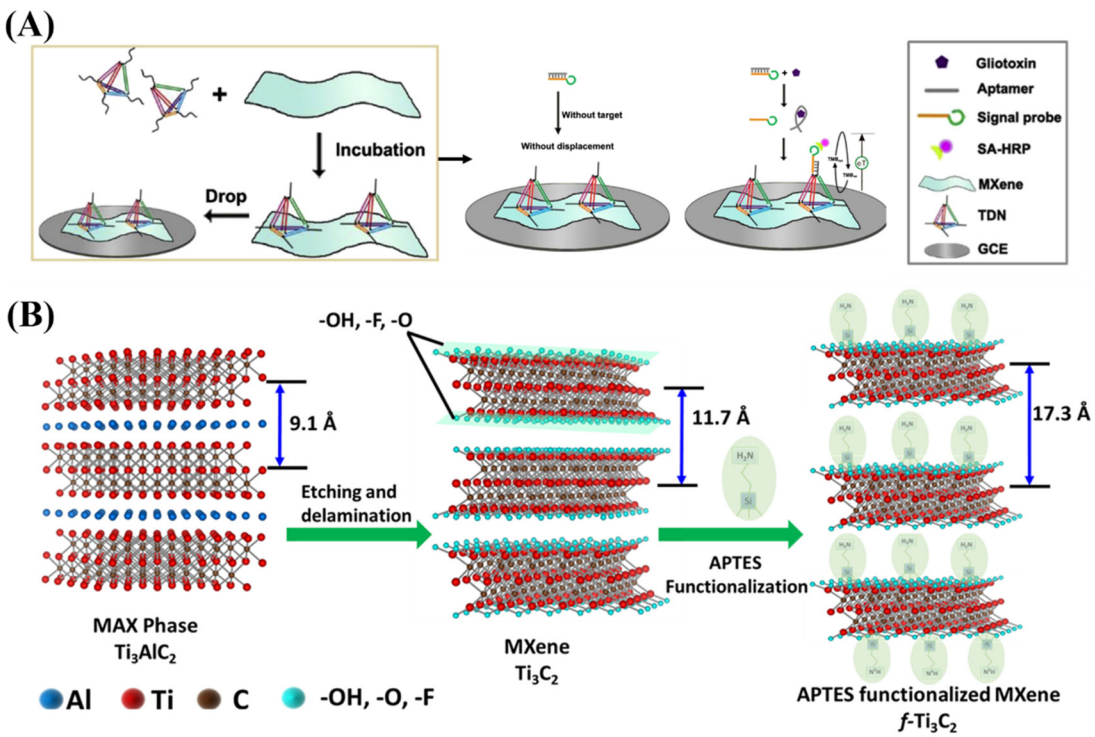

Fig. 5 (A) Schematic illustration of the preparation of the TDN/MXene modified electrode and the principle of the TDN/MXene-based electrochemical sensor for gliotoxin detection. Reproduced from ref. 40 with permission from ELSEVIER, copyright 2019. (B) Schematic illustration of Ti_3C_2-MXene functionalization. The aluminum layer is etched from the Ti_3AlC_2-MAX phase, which delaminates into 2D nanosheets; the sheets consist of two layers of carbon sandwiched between three layers of titanium with the surface of titanium randomly terminated with −OH, −O, and −F functional groups. Aminosilane (APTES) is then used to functionalize the Ti_3C_2-MXene surface. Reproduced from ref. 41 with permission from ELSEVIER, copyright 2018.

modifications. The TDNs act as rigid scaffolds to maintain suitable orientation, enhancing molecular recognition and signal amplification on the electrode. Additionally, the gliotoxin aptamer further improves the efficient and cost-effective detection of the analyte.[40] In addition, surface modification and functionalization can improve the biocompatibility of MXenes. Since the original surface of MXenes is chemically active, their surface functional groups may sometimes be unsuitable for direct contact with certain biological samples. The incorporation of biocompatible materials with favorable biocompatibility through surface modification can enhance the biocompatibility of MXenes, rendering them suitable for prolonged utilization in biosensors and circumventing the potential cytotoxicity and allergic reactions that may arise from direct exposure. Because of the existence of –OH terminal groups, MXenes can be functionalized using silylation reagents to produce MXene nanosheets patterned with amino silane moieties (Fig. 5B). This modification enables NHS/EDC-based amine coupling, allowing for the covalent immobilization of receptors, such as antibodies.[41] Jiang *et al.* introduced an FM-Exo hydrogel, a blend of MXenes and M2 macrophage exosomes, which enhances diabetic wound healing by counteracting immunosuppression caused by high glucose. This strategy holds promise for treating diabetic wounds and other inflammation-related tissue repairs using MXene-based biosensors.[42] Therefore, through surface functionalization, the chemical and physical stability of MXenes can be significantly improved, especially in the complex environment of biological samples; surface modification can also reduce interference, prevent non-specific adsorption, and enhance the long-term stability of the sensor.

The primary surface modification and functionalization strategies for MXenes include the introduction of functional groups, modified polymers, metal nanoparticles and other nanomaterial composites. Firstly, the introduction of functional groups represents a common approach for surface modification of MXenes, which naturally exhibit functional groups such as hydroxyl (–OH), oxygen (–O) and fluorine (–F) groups, which provide strong chemical activity and are capable of binding to a wide range of biomolecules (antibodies, DNA, enzymes, *etc.*). Further modification of these functional groups can result in a notable enhancement of MXenes' ability to bind biomolecules. For instance, the incorporation of a carboxyl group (–COOH) can augment the affinity with biomolecules, particularly between antibodies and antigens,[43] and enhance the sensitivity of electrochemical sensors. On the other hand, the introduction of an amino ($-NH_2$) group enhances the binding ability of MXenes[44] with negatively charged biomolecules (*e.g.*, DNA and RNA), thereby improving performance in areas such as genetic testing. Furthermore, the incorporation of a sulfur (–SH) group facilitates the interaction of MXenes with biomolecules,[45] including metal ions and proteins, thus enhancing the selectivity and sensitivity of the sensor. Secondly, polymer modification is another effective strategy to improve the biosensing performance of MXenes. By modifying polymers such as polyvinyl alcohol (PVA), polypyrrole (PPy), or polyethyleneimine (PEI) onto the surface of MXenes, it is possible to effectively improve their biocompatibility and modulate their hydrophilicity, conductivity, and stability. For example, the modification of PVA can improve the biosolubility and stability of MXenes,[46] while the modification of polypyrrole[47] enhances the electrochemical response and improves the efficiency of signal transmission. PEI-modified MXenes[48] exhibit strong binding capability for detecting biomolecules like DNA and proteins, thereby boosting sensor signal strength. Additionally, modifying MXenes with metal nanoparticles (such as gold, silver, or copper) is a common approach to enhance biosensor performance. The catalytic properties of these metals, along with the surface plasmon resonance (SPR) effect, can improve electrochemical signals, leading to increased sensitivity of the sensor. In electrochemical detection, metal-modified MXenes can accelerate the reaction of target molecules and enhance the signal change.[49] In addition, the composite of MXenes with carbon-based nanomaterials (graphene, carbon nanotubes, *etc.*) can enhance the electrochemical sensing performance by increasing the electrical conductivity, increasing the specific surface area, and improving the biomolecule adsorption ability. Metal oxide (*e.g.*, ZnO, CuO, and TiO_2) modification can enhance the potential of MXenes for photocatalysis and biosensing applications, especially in the detection of heavy metal ions and DNA analysis. Although significant progress has been made in the surface modification of MXenes for biosensing applications, there is still a long way to go before real-time biosensing becomes a reality.

3. Advantages of MXenes as biosensing materials

Compared to conventional sensing materials (metal oxides, graphene, carbon nanotubes, and conductive polymers), MXenes exhibit significant advantages, which are mainly in the areas of electrical conductivity, mechanical properties, multifunctionality, and processability. Firstly, MXenes exhibit high electrical conductivity, with values ranging from 850 to in excess of 20 000 S cm^{-1},[10,11,50] which can be attributed to the weak bonding between the transition metal layers (*e.g.* Ti, Nb, and Ta) and the carbon or nitrogen layers of MXenes. In this structure, the d-electron clouds of the transition metal atoms permit MXenes to readily conduct electricity in the presence of an electric field, thereby achieving electrical conductivity that is often comparable to, or even exceeds, that of many metallic materials. In comparison, the intrinsic conductivity of metal oxides is typically below 10^{-1} S cm^{-1}, and the majority of these materials require doping or external stimulation (*e.g.*, heating or application of an electric field) to achieve significant improvements in conductivity properties. For example, titanium dioxide (TiO_2) has a very low intrinsic conductivity (10^{-12}–10^{-8} S cm^{-1}) and is usually an insulator or a wide-bandwidth semiconductor, which can be improved by doping (*e.g.*, nitrogen, fluorine, or transition metals).[51] The electrical con-

ductivity of a material depends on the mobility and density of charge carriers. Graphene has the potential to function as an excellent conductor; however, the development of macroscopic graphene materials with optimal electrical properties remains a significant challenge. Furthermore, the high electron mobility of graphene is contingent upon its structural integrity and substrate.[52] The majority of reported graphene (or graphene derivatives) reinforced metal matrix composites have demonstrated electrical conductivity that is not superior to that of pure metal matrix composites.[53–55]

Although carbon nanotubes are also potential two-dimensional nanomaterials for biosensing, MXenes are considered superior due to their larger surface area, enhanced electrical conductivity, more versatile surface chemistry, and hydrophilicity, which renders them more compatible with biological environments. While CNTs are mechanically robust and stable, MXenes demonstrate superior resilience to heat and chemicals, rendering them optimal for biosensing in humid environments.[56] Conducting polymers (polyaniline, polypyrrole, polyacetylene, *etc*.) typically have low electrical conductivity and need to be doped or modified to significantly enhance the conductivity. Conductive polymers offer significant advantages in the field of flexible and transparent electrodes; however, they exhibit lower conductivity and stability than MXenes. Secondly, the numerous surface functional groups of MXenes can be chemically modified to bind to target molecules, metal nanoparticles or polymers, thereby enhancing the selectivity and stability of the sensors. For example, hydroxyl (–OH) and oxygen (–O) groups can effectively improve the surface hydrophilicity of MXenes,[57] and these groups can also facilitate catalytic processes in electrochemical reactions. Furthermore, these surface functional groups are capable of interacting with charge vectors, thereby optimizing the carrier transport paths and thus enhancing the electrical conductivity. This confers significant advantages upon MXenes in the context of electronic devices, sensors and energy storage. In energy storage devices such as supercapacitors[58] and lithium-ion batteries,[59,60] MXene electrode materials facilitate rapid electron transfer, thereby enhancing charge and discharge rates and energy density. In contrast, materials such as graphene typically require complex chemical modifications to achieve comparable results.

The high specific surface area of MXenes is also a remarkable property of the material, and this property brings great advantages in a variety of applications, especially in energy storage,[61] catalysis,[62] sensors,[63] and environmental remediation.[64] The two-dimensional structure of MXenes endows them with an exceptionally high specific surface area, which is markedly larger than that of conventional three-dimensional materials. The 2D structure of the material allows each atom to be exposed to the surface, thereby facilitating greater involvement of surface atoms in the reaction and adsorption processes of the substance, which in turn increases the active surface area. The presence of additional surface sites enables the storage and transfer of charge over a more extensive area, thereby enhancing the efficiency and power density of energy storage devices.[65] Furthermore, the hydroxyl (–OH) and oxygen (–O) groups on the surface of MXenes can enhance the chemical reactivity and affinity of MXenes, enabling them to interact with a wide range of molecules and ions, thus providing additional adsorption sites. In catalytic reactions,[66,67] the reactants typically interact with the catalyst's surface, meaning that an increased surface area directly enhances catalytic efficiency. The high specific surface area of MXenes allows them to adsorb more reactant molecules, offering more active sites and thereby boosting the catalytic rate. Additionally, MXenes can be employed as gas sensing[68,69] materials for the identification of noxious gases, including ammonia, nitrogen dioxide, and nitrogen oxides. The provision of additional adsorption sites enables MXenes to markedly enhance the sensitivity and response speed of gas detection. In water treatment,[70,71] the high specific surface area of MXenes enables the effective removal of heavy metal ions and organic pollutants from water. The adsorption of contaminants by MXenes facilitates the purification of water and mitigates the risk of water pollution.

MXenes also exhibit favorable mechanical flexibility and ductility, enabling them to adapt to bending or stretching environments. This is mainly due to the lamellar structure and interlayer interactions of MXenes themselves, endowing them with superior elasticity and ductility under stress.[72] Consequently, the weak interactions between the layers permit the slippage of MXenes when subjected to external forces, preventing fracture or disintegration. MXenes exhibit enhanced toughness and greater deformability when subjected to tensile or compressive forces than conventional brittle materials. This indicates that MXenes are capable of maintaining stability in high-stress environments and of efficiently absorbing mechanical energy in order to prevent rupture. Li *et al.* developed a self-powered piezoelectric sensor with an electrolyte layer and MXene/AgNP electrodes. The 2D MXene nanosheets offer abundant ion channels, while AgNPs prevent self-stacking, allowing the sensor to generate a high voltage of 11.1 mV at 0.7% strain. It shows excellent stability, maintaining 95% of its signal after 13 000 seconds of cyclic bending. Additionally, the sensor can be attached to a glove to produce electrical signals in pulse or square wave form through finger movements, enabling information transmission *via* the Morse code.[14] The functional groups present on the surface of MXenes, including the hydroxyl (–OH) and oxygen (–O) groups, not only facilitate electrochemical reactions but also influence the mechanical properties of MXenes. Functional groups also can enhance the interfacial bonding between MXenes and other materials, especially in composites, and enhance their mechanical stability. This renders it an optimal material for flexible and wearable sensors, whereas metal oxides frequently encounter difficulties in meeting such requirements due to their inherent brittleness. For example,[73] the incorporation of MXenes into polymer, metal or ceramic matrices can significantly improve the strength, toughness and wear resistance of composite materials. In particular, within the aerospace and automotive industries, where high performance is a prerequi-

site, MXene composites are capable of reducing the weight of the materials while simultaneously increasing their strength.[74] The Ti_3C_2 MXene is used as a toughening and reinforcing agent in carbon fiber-reinforced composites which exhibit high tensile strength and impact resistance. MXenes are employed extensively in flexible electronic devices[75] due to their high toughness and ductility. For instance, in devices such as flexible supercapacitors,[76] batteries,[77] and sensors,[78] MXene electrode materials are capable of withstanding repeated bending and stretching without compromising their electrical conductivity and structural stability. The Ti_3C_2 MXene retains its superior electrochemical properties after repeated mechanical stretching, making it an optimal material for flexible electronic devices.[79] Furthermore, its wet processability (film formation and fibrillation) is superior, rendering it suitable for the industrial preparation of thin film and fiber sensors. In comparison, materials such as carbon nanotubes are more challenging to process. Collectively, MXenes demonstrate considerable potential as sensing materials in the domain of biosensors, combining high electrical conductivity, chemical versatility, mechanical flexibility, and processability. This compensates for the limitations of traditional materials.

4. MXenes as biosensors

The advancement of biosensors is inextricably linked to the development of newer generations of biosensing materials, particularly the emergence and enhancement of nanomaterials. Nanomaterials applied to sensors should exhibit high conductivity, a high specific surface area, good mechanical strength, and potential biocompatibility. Given that MXenes have already demonstrated excellent electrochemical properties in supercapacitors and batteries. Moreover, the inherent characteristics of MXene materials align well with the performance requirements for biosensor applications. As a result, researchers have increasingly leveraged the exceptional electrochemical properties of MXene-based nanocomposites to develop innovative biosensing platforms. This section will focus on the application of MXenes in the development of biosensors.

4.1. MXene based electrochemical biosensors

Electrochemical sensors represent the most prevalent category of biosensors. Given that MXenes have already exhibited noteworthy electrochemical functionality in supercapacitors,[80–82] batteries,[83–85] and other domains, they are promising candidates for biosensor development. Consequently, there has been a notable increase in the development and application of MXene biosensors.

4.1.1. MXene based sensors for cancer biomarkers. The presence of cancer markers is crucial for the early diagnosis and monitoring of cancer. However, during the early stages of cancer or in small tumors, these markers are often present at extremely low concentrations, which can hinder their detection during early screening. It is possible that numerous markers may not attain sufficient concentrations in the early stages of cancer or when tumors are small. This may result in a reduction in the sensitivity of the assay and the failure to identify the optimal time for treatment. Some highly sensitive assays (such as mass spectrometry and nucleic acid amplification techniques) require expensive equipment and complex operations, which limits their widespread use in clinical settings, particularly in resource-limited areas. The sensitivity of the monitoring range and the cost of monitoring are crucial indicators for the timely treatment of cancer. MXenes can selectively capture cancer markers through surface modification with various biomolecules, including antibodies, DNA probes, and other biomolecules. When the MXene surface is modified with a specific antibody, the electrochemical signal undergoes a change when the target molecule (*e.g.* tumor marker) binds to the MXene surface. This enables the sensor to detect the cancer marker in a rapid and sensitive manner. Zare *et al.* designed an electrochemical aptasensor platform for the accurate detection of HER2, a critical biomarker linked to breast cancer. The sensor was fabricated by functionalizing TiVC-MXene nanosheets with gold nanoparticles, followed by the immobilization of thiolated HER2 aptamers loaded with Pb^{2+} ions onto the electrode surface. Subsequently, the HER2-specific aptamer was attached to the surface of SPCE/TiVC-MXene/Au NPs *via* a covalent bond between the Au NPs and the thiolated aptamer. The presence of Au NPs ensured the high conductivity of the aptasensor and effective binding of the aptamer to the surface of the SPCE/TiVC-MXene, as well as enlarging the active surface of the biosensor. The large surface area of the TiVC MXene significantly improves the biosensor's conductivity and enhances aptamer loading efficiency for biomarker detection. Upon HER2 binding, the aptamer selectively interacts with the target, reducing its affinity for Pb^{2+} ions. This leads to an increase in free Pb^{2+} concentration and peak current, enabling accurate HER2 monitoring.[86] Sanjayan *et al.* used EDC-NHS chemistry to functionalize MXene nanosheets (MNSs) with carcinoembryonic antigen (CEA) antibodies after increasing the layer spacing of MXene nanosheets by hydrothermal treatment to form MNS-CEA Abs (Fig. 6). The formation of biocoupling between CEA antibodies and MNSs markedly improves the selectivity of electrochemical biosensors for CEA biomarkers.[87] Subsequently, the charge transfer characteristics and resistance alterations at the electrode interface are examined through the utilization of cyclic voltammetry (CV) and impedance analysis, thereby facilitating the precise identification of cancer biomarkers within clinical specimens.

4.1.2. Glucose sensors. The principal function of a sensor for the monitoring of diabetes[88] is the detection of the blood glucose concentration in blood or tissue fluids, followed by the conversion of this data into an electrical signal for real-time monitoring by medical professionals or patients. However, existing sensors are prone to errors, particularly at very low or very high blood glucose concentrations. The popularity of these sensors has been constrained by a number of factors, including their susceptibility to external influences, shorter

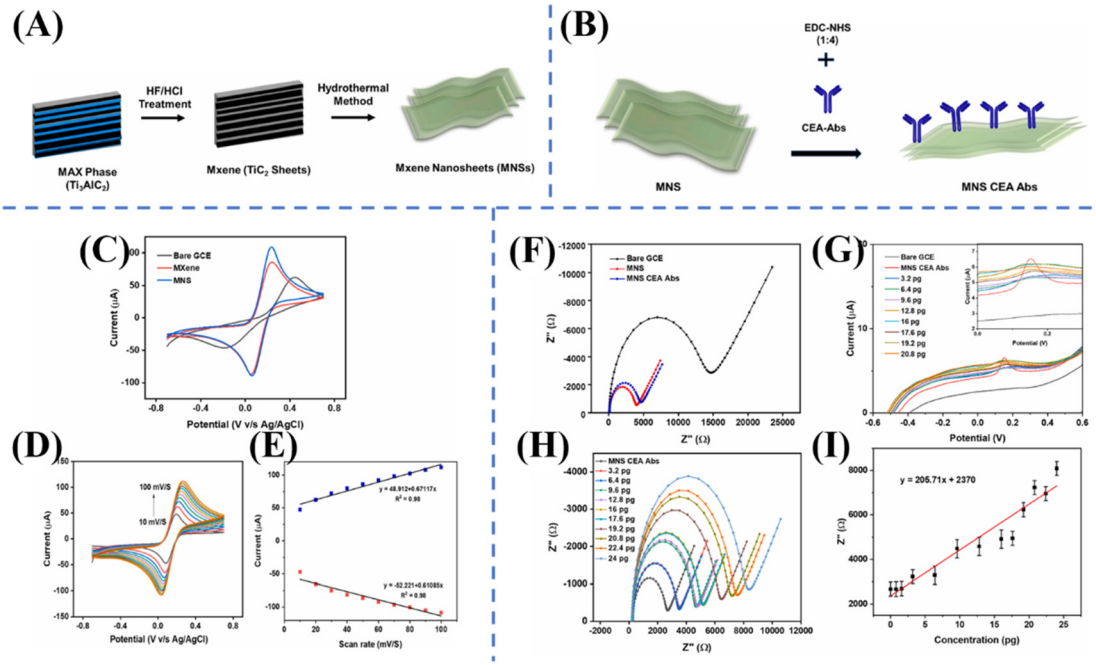

Fig. 6 (A) Schematic illustration of the synthesis of MXene ($Ti_3C_2T_x$) nanosheets by using the hydrothermal method. (B) Functionalization of MNSs with CEA Abs. (C) CV curves of the bare GCE, MXenes, and MNSs at a scan rate of 50 mV s^{-1}. (D) Scan rate study of MNSs. (E) Linear plot of the change in oxidation and reduction current *vs.* scan rate. (F) EIS spectra of the bare GCE, MNSs, MNS CEA Abs, and MXenes. (G) CV curves of MNS CEA Abs with an increase in the CEA biomarker analyte. (H) EIS response of MNS CEA Abs upon addition of the CEA biomarker analyte. (I) Linear plot of EIS response MNS CEA Abs *vs.* the CEA biomarker analyte. Reproduced from ref. 87 with permission from ELSEVIER, copyright 2025.

lifespans, and higher costs. Two-dimensional nanomaterial MXenes have the potential to address these issues to a certain extent. Bian *et al.* electrodeposited a layer of conical gold nanostructures (AuTNs) with MXenes coated on a glassy carbon electrode (GCE). As shown in Fig. 7, the high surface area ratio of AuTNs on the MXene layer could increase the number of active sites and allow easy adsorption of glucose molecules. Due to the high conductivity of the MXene layer, the transfer of electronic charge from AuTNs to GCE is accelerated during glucose oxidation. By analyzing the current density of the oxidation peak and the current difference based on the pulse potential during the electrochemical process, the concentration of glucose can be accurately monitored by the CV test and DPV test. The modified AuTNs/MXene/GCE electrode has a wide linear range, a low detection limit (0.1 nM), and a fast response time (1.0 s). In healthy individuals, acetone levels in breath are typically below 1 ppm (ranging from 0.3 to 0.9 ppm), whereas they rise to 2.7 ppm and 2 ppm in patients with type 2 and type 1 diabetes,[89] respectively. Hence, detecting acetone concentrations at sub-ppm or even ppb levels is essential for the early diagnosis of diabetes.[90] Breath-based biosensors have the advantage of being non-invasive and easily reproducible, unlike the cumbersome nature of blood and urine tests. Ruide *et al.* utilized CrWO/MXene nanocomposites as the sensing material in a chemo-resistive sensor. The semiconductor material reacts with acetone in the air and produces resistance changes related to acetone levels. Due to the two-dimensional composite structure, huge surface and interfacial surfaces and abundant active sites. The highest sensitivity to 2.86 ppm acetone at room temperature is achieved with a detection limit of 0.1 ppm.[91] Siraj *et al.* prepared a $MoS_2/Ti_3C_2T_x$ material and a contact-type flexible and highly selective acetone gas biosensor based on the $MoS_2/Ti_3C_2T_x$ material. The biosensor demonstrated a high level of sensitivity (R = 5.84%) to acetone concentrations ranging from 5 to 30 ppm at room temperature.[92]

4.1.3. MXene based sensors for environmental contaminants. Due to their high surface area and exceptional electrical conductivity, MXene materials are extensively applied in environmental contaminant detection. MXene-based biosensors are particularly effective for monitoring environmental factors like water and air quality, with a focus on detecting heavy metal ions[93,94] and toxic gases.[95] Given that MXene surfaces can chemically bind or electrostatically interact with these metal ions,[96] they can be employed as electrochemical sensor materials to detect metal ion concentrations through electrochemical reactions, including cyclic voltammetry and differential pulse voltammetry. For example, Ti_3C_2 MXene materials are used to detect Cd^{2+} and Pb^{2+} ions,[97] and the change in their electrochemical signals can be used to quantify the concentration of lead ions in water. Lead contamination is linked to severe health issues, such as central nervous system damage, anemia, kidney dysfunction, and cognitive and behavioral impairments.[98] Blood lead levels are currently the most reliable indicator of health risks from exposure. In a recent study, Au NPs (AuNP)-$Ti_3C_2T_x$ hetero-

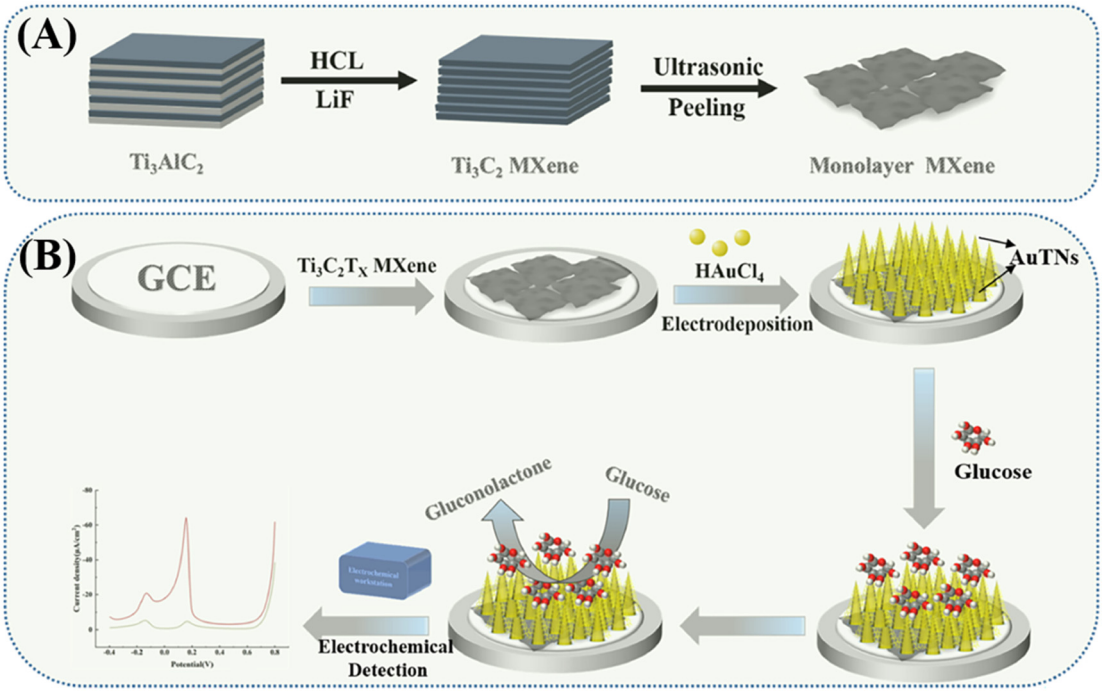

Fig. 7 (A) Large scale fabrication of MXene single layers. (B) The mechanism of glucose detection with a modified electrode of AuTNs/MXene/GCE. Reproduced from ref. 89 with permission from ELSEVIER, copyright 2024.

structures were employed as anode materials (Fig. 8), while Co, Mn–N-doped carbon nanosheets served as cathode catalysts to create a self-powered, enzyme-free biofuel cell (BFC-SPS) for lead ion detection in human plasma. This BFC-SPS demonstrated remarkable stability, selectivity, and effectiveness in detecting Pb^{2+} in plasma.[99] Similarly, mercury ions (Hg^{2+}) can bind specifically to sulfur groups (–SH) on MXene surfaces, enabling highly sensitive electrochemical detection of mercury.[100]

In addition to heavy metal ions, MXenes have also been employed for monitoring organic pollutants in water. Through the modification of surface functional groups, MXenes can effectively adsorb benzene,[101] phenolic compounds,[102] pesticides and other organic pollutants,[103] This makes it an ideal material for use in environmental water quality monitoring and water purification,[104] thus providing a healthy living environment for organisms. Therefore, MXene materials also hold great potential in biosensors for environmental monitoring.

4.1.4. MXene based gas sensors. Gas sensors have a wide range of applications in respiratory monitoring, diagnostics, therapeutics and toxic gas monitoring.[105,106] MXenes can be used to design gas sensors with high sensitivity and selectivity by adsorbing gas molecules and changing their electrical or electrochemical properties. Nitrogen dioxide (NO_2) is a highly hazardous irritant gas. Prolonged inhalation of this substance can lead to lung organ disease and an increased susceptibility to respiratory infections. Those with underlying respiratory conditions, the elderly and children are particularly susceptible to the effects of NO_2 exposure. Le *et al.* engineered Ti_3C_2-MoS_2 composites by integrating 2D MXenes with MoS_2, achieving high conductivity and surface functionalization. The Ti_3C_2 MXene surface, enriched with active terminal groups (–OH, –F), interacts with atmospheric O_2 molecules, partially catalyzing their decomposition into atomic oxygen (O). These oxygen species, along with residual O_2, extract electrons from MXenes *via* surface terminations, generating oxygen ions (O^{2-}/O^{-}) anchored on the material. Concurrently, the MoS_2 component physisorbs NO_2 molecules, which exhibit strong electrophilicity and readily capture electrons from the composite. The intimate interfacial contact between MoS_2 and MXenes facilitates the migration of oxygen ions (O^{2-}/O^{-}) to MoS_2, where they supply electrons to adsorbed NO_2. This electron transfer mechanism induces measurable resistance changes, enabling real-time NO_2 monitoring.[107] Another report demonstrated that a novel gas sensor based on rGO/MXenes[108] exhibited a sensitive and reproducible response to NO_2 attributed to their abundant active surface sites, excellent conductivity, and expansive surface area. Furthermore, the rGO/$Ti_3C_2T_x$ heterostructure exhibits response signals to additional toxic gases, including CH_4 and C_7H_8. This suggests that it could be a promising material for sensing a range of toxic gases.

4.1.5. MXene based electrochemical wearable biosensors. Wearable portable sensors represent a crucial element in the development of wearable medical and health monitoring products, offering significant potential for advancing research in this field. As shown in Fig. 9A and B, wearable portable sensors are distinguished by their exceptional flexibility, which allows for the utilization of flexible conductive fibers as electroactive components.[109] The flexibility and malleability of

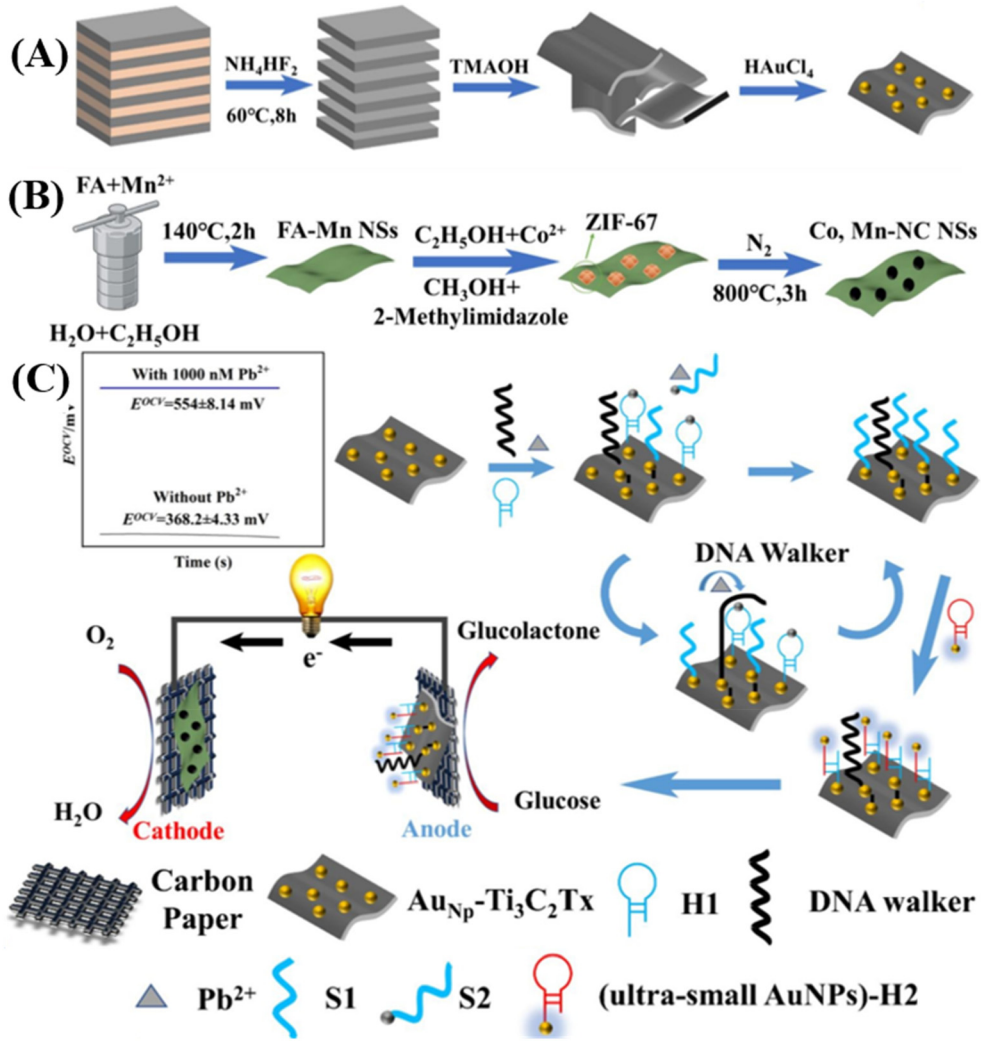

Fig. 8 (A) AuNp-$Ti_3C_2T_x$ heterostructures, (B) Co, Mn-NC NSs and (C) schematic diagram of BFC-SPS for the detection of Pb^{2+}. Reproduced from ref. 99 with permission from ELSEVIER, copyright 2024.

MXenes make them ideal materials for the fabrication of flexible fiber sensors and thin-film sensors. As the fibers are flexible, knittable, and easy to integrate, the preparation of MXenes in fiber form for wearable portable sensors can greatly enhance the universality and convenience of the sensors. Wang *et al.* proposed a layered sensing fiber based on the principle of electrostatic adsorption and hydrogen bonding interactions (Fig. 9C), where MXene/thermoplastic polyurethane (TPU) composite fibers with high strain were obtained by wet spinning, and then polypyrrole (PPy) was coated on the surface of the composite fibers. Finally, the fibers were encapsulated for protection. The hierarchical fiber strain sensor boasts an impressive gauge factor (ranging from 60 to 3.23×10^6) and wide sensing range (0–10^6%), with excellent stretchability (>750%) and a modulus of 12 MPa.[110] This sensor can monitor real-time deformations in various body joints during physical activity, track leg swelling in varicose vein patients, and exhibit significant Joule heating effects, paving the way for advancements in multifunctional intelligent biosensors. Because it has a large surface area, the film can receive and transmit monitoring signals in a large range, quickly and sensibly, and can also greatly improve the sensitivity of wearable portable sensors. In a recent study, Zhang *et al.* successfully fabricated a wearable MXene-based respiratory sensor and integrated it into a mask (Fig. 9D–H). The sensor employs the thermoelectric effect of the MXene/CNT/PEDOT : PSS composite film to generate a voltage signal based on the Seebeck effect, which is used to monitor the respiration rate of an organism.[111] Furthermore, the sensor displays considerable potential for use in EMI shielding and self-heating applications. When integrated with heart rate monitoring, it becomes a viable tool for real-time human health monitoring.[112,113] Table 2 summarizes the applications of MXene composite materials in the field of sensing.

4.2. MXene based optical biosensors

MXenes provide a new strategy for optical biosensing by virtue of their broad spectral absorption,[114] high photothermal con-

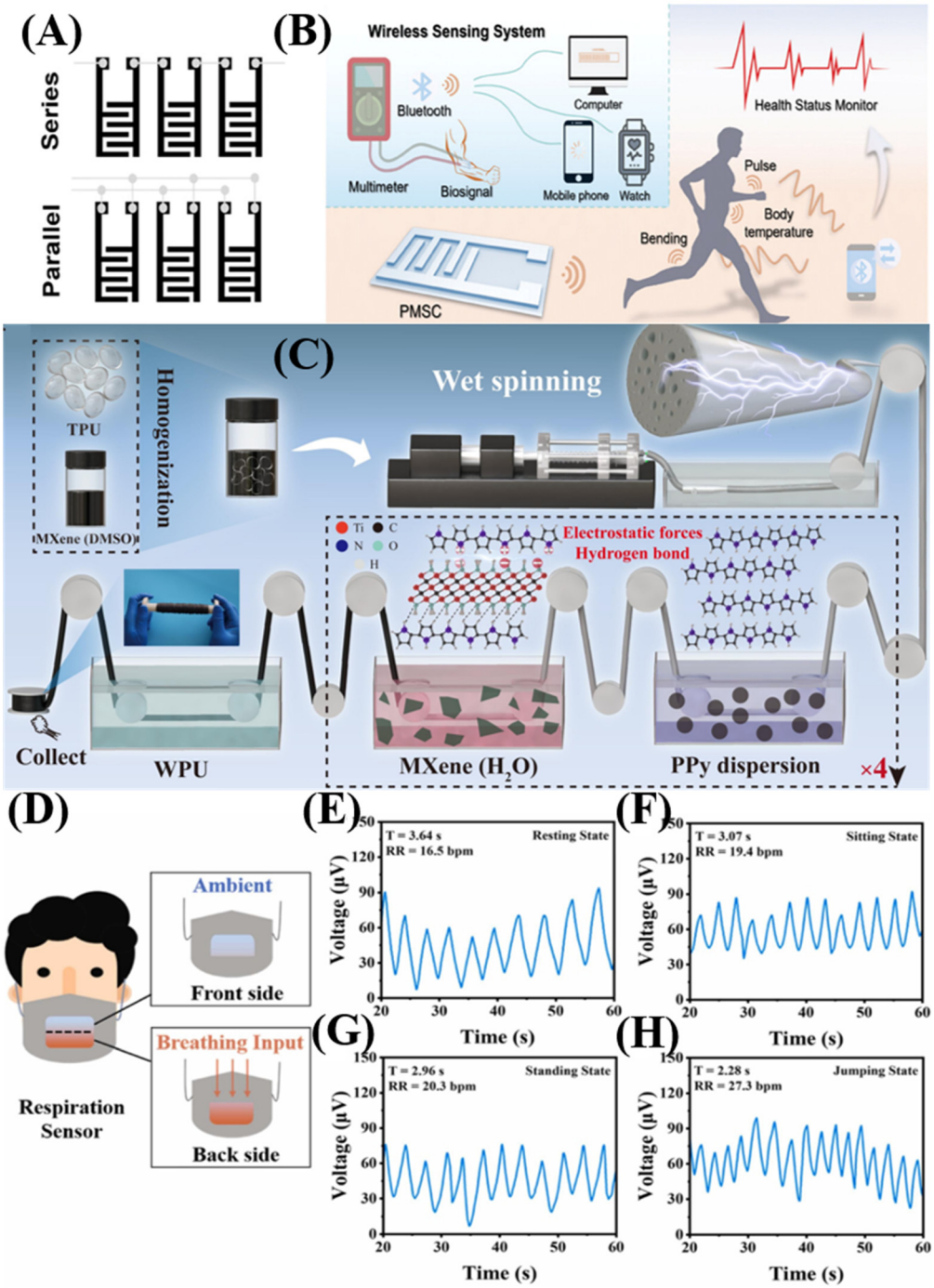

Fig. 9 (A) Schematic illustration of PMSCs connected in series and parallel. (B) Schematic diagram of the PMSC-based wireless sensing system for monitoring the bending, pulse, and temperature signals. Reproduced from ref. 109 with permission from WILEY, copyright 2024. (C) Schematic diagram of the preparation process of the hierarchically structured fiber strain sensor. Reproduced from ref. 110 with permission from ELSEVIER, copyright 2024. (D) Integration of a respiration sensor into a facial mask with the back side near the breathing input and the front side exposed to air. (E–H) Respiration signals sensed in resting, sitting, standing and jumping modes. Reproduced from ref. 111 with permission from ELSEVIER, copyright 2023.

version efficiency,[115,116] surface plasmon resonance (SPR)[117,118] properties, and abundant surface functional groups.[119,120] Sun *et al.* developed a hydrogel by incorporating MXene nanosheets into a polyampholyte matrix of dimethylaminoethyl acrylate quaternized ammonium (DMAEA-Q) and NaSS. The resulting EPAM hydrogels displayed excellent infrared imaging performance and cycling stability under light exposure. The photothermal conversion mechanism, driven by MXenes' localized surface plasmon resonance (LSPR) effect, generates photothermal electrons that produce measurable

Table 2 Sensing applications of MXenes

Material	Target	Linear range	Limit of detection	Ref.
SPCE/TiVC-MXene/Au NPs/Pb^{2+}-aptamer	HER2	1.0–1200 pg mL^{-1}	50 fg mL^{-1}	86
MNS CEA Abs	CEA	1–25 pg mL^{-1}	3.2 pg mL^{-1}	87
AuTNs/MXene/GCE	Enzyme-free glucose	0.1 nM–10.0 mM	1.43 nM	89
MXA-CuO/CC	Cd^{2+}/Pb^{2+}	4 μg L^{-1}–800 μg L^{-1}/4 μg L^{-1}–1200 μg L^{-1}	0.3 μg L^{-1}/0.2 μg L^{-1}	97
Au NPs-$Ti_3C_2T_x$	Pb^{2+}	0.01–7500 nM	0.43 pM	99
MXene-GSH	Hg^{2+}	140–540 nM	1.16 nM	100
GCE/$Ti_3C_2T_x$-Fe_2O_3	Hydrogen peroxide	10–1000 nM	7.46 nM	111
PEI-Ru@Ti_3C_2@AuNPs	SARS-CoV-2 RdRp gene	0–500 × 10^{-9} nM	12.8 nM	112

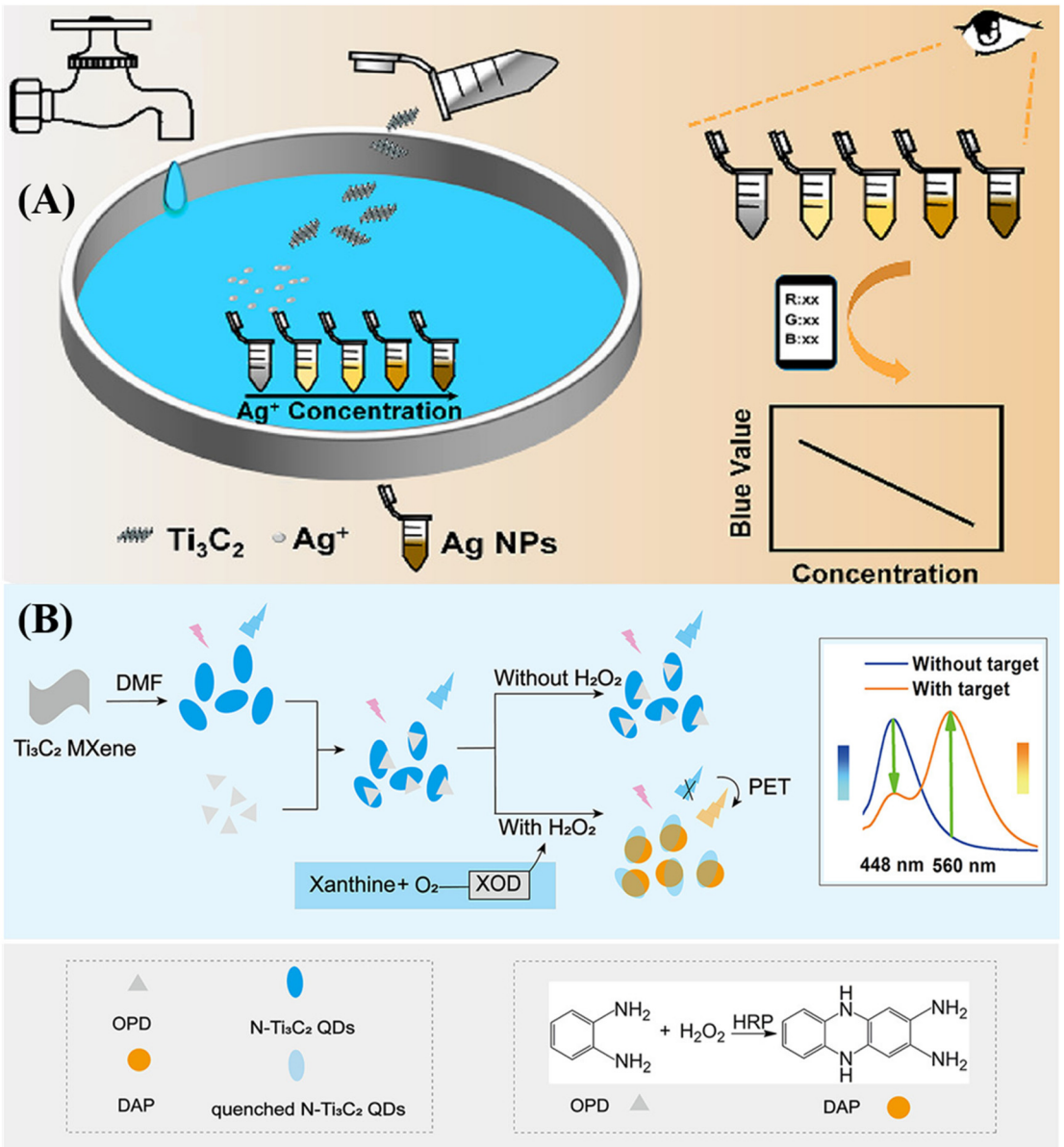

Fig. 10 (A) Principles of a label-free and visualised nanoplasma strategy for silver ion sensing. Reproduced from ref. 122 with permission from American Chemical Society, copyright 2020. (B) Schematic illustration of a ratiometric fluorescence strategy for the detection of H_2O_2 and xanthine. Reproduced from ref. 124 with permission from American Chemical Society, copyright 2020.

temperature signals, highlighting the sensor's reliability and stability. Furthermore, the photoresponsive sensor exhibits self-healing and swelling resistance, paving the way for the development of next-generation MXene-based photoresponsive sensors.[121]

4.2.1. MXene based colorimetric biosensors. MXenes are highly suitable for colorimetric biosensors due to their exceptional properties, such as facile functionalization, large surface area, hydrophilicity, and superior conductivity. As shown in Fig. 10A, Wang *et al.* designed a label-free colorimetric sensor based on Ti_3C_2 MXene-polyacrylic acid (PAA) composites for Ag^+ detection. The sensor demonstrated remarkable stability in aqueous solutions and efficiently reduced Ag^+ ions, leading to a visible color change that enabled quantitative Ag^+ analysis with a detection limit of 615 nM, making it suitable for rapid Ag^+ screening in drinking water.[122] In another study, Li *et al.* utilized a NiFeLDH-modified Ti_3C_2 MXene as a nanozyme to catalyze the oxidation of 3,3′,5,5′-tetramethylbenzidine (TMB), resulting in a distinct blue color change for glutathione detection.[123]

4.2.2. MXene based fluorescent biosensors. MXenes exhibit significant potential in fluorescence detection owing to their excellent dispersibility and distinct optical characteristics. For instance, $Ti_3C_2T_x$ quantum dots (ranging from nanometers to tens of nanometers in size) demonstrate tunable luminescence upon photon excitation, whereas $Ti_3C_2T_x$ nanosheets display broad-spectrum light absorption.[124] Enhanced doping strategies and scalable synthesis of MXene quantum dots further amplify their applicability in high-sensitivity fluorescence sensing platforms (Fig. 10B). After surface modification of MXenes using amino groups on the surface of polyethyleneimine, Chen *et al.* made it possible to deprotonate or protonate at different pH values. The pH-responsive Ti_3C_2 quantum dots produced a fluorescence peak at 460 nm due to electron localisation. In contrast, pH-responsive $[Ru(dpp)_3]Cl_2$ exhibited fluorescence intensity at 615 nm.[125] A ratiometric MXene-based photoluminescence sensor was engineered by integrating dual fluorescence systems, enabling precise pH estimation within intracellular organelles. The sensor demonstrated outstanding biocompatibility and negligible cytotoxicity, making it highly suitable for biological applications. In another study, an efficient fluorescent sensor using an ultra-thin Ti_3C_2 MXene as a fluorescent bursting agent was reported for quantitative screening of mercury in rivers and tap water.[126]

4.2.3. MXene based electrochemiluminescent sensors. Electrochemiluminescence measures the target analyte concentration by correlating it with the intensity of light emitted during redox reactions of luminescent molecules generated electrically.[127] MXenes' high conductivity and reactivity enhance the redox efficiency of the luminophore and accelerate electron transfer, ultimately improving the sensitivity of the electrochemiluminescence system. Zhang *et al.*[128] utilized aptamer-modified Ti_3C_2 MXene nanoprobes for the detection of Michigan Cancer Foundation-7 (MCF-7) exosomes, which enhances the redox reaction of the luminophore and boosts photoemission (Fig. 11). Meanwhile, Sun *et al.* developed a highly sensitive electrochemiluminescent sensor for glucose detection at nanomolar concentrations using a Ti_3C_2 MXene-TiO_2 platform. By immobilizing glucose oxidase onto the surface, they catalyzed the conversion of glucose to hydrogen peroxide, amplifying the electrochemiluminescence signal and enabling precise glucose monitoring.[129] As we mentioned earlier, Zhang *et al.* designed electrochemiluminescent bio-

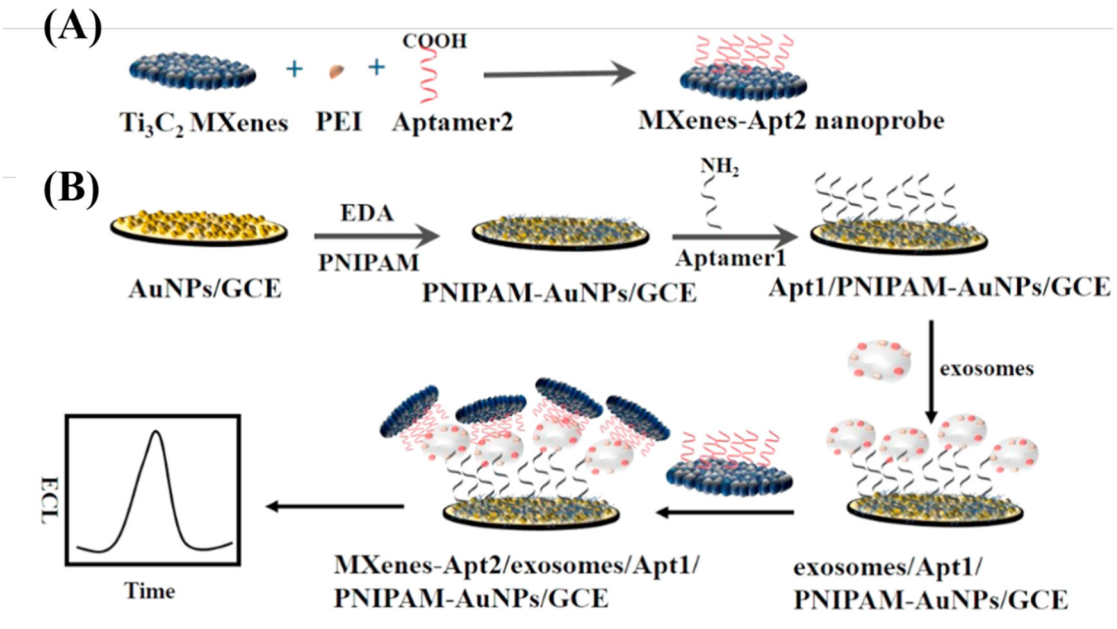

Fig. 11 (A and B) The principle of the ECL biosensor for the exosome activity detection signal amplification strategy. Reproduced from ref. 128 with permission from ELSEVIER, copyright 2019.

sensors for COVID-19 diagnosis and monitoring. Their method involved using a three-dimensional DNA walker to amplify double-stranded DNA, which in turn activated CRISPR-Cas12a. This activation cleaved single-stranded DNA on the Ti_3C_2 MXene-coated sensor surface, causing the ferrocene-modified DNA to separate from the surface and significantly increase the electrochemiluminescence signal.[113]

5. Challenges and future perspectives

Despite the numerous advantages of MXene materials in the field of biosensors, several challenges remain. These challenges extend beyond the inherent properties of the MXene materials and encompass their application in complex biological samples, the optimization of sensor systems, and the resolution of large-scale production issues.

The primary challenge associated with MXenes with regard to material stability pertains to their tendency to undergo hydration and oxidation. Untreated MXenes are susceptible to reaction with water in air or water dispersion, resulting in surface oxidation and the formation of TiO_2 oxide films and particles. Typically, MXene materials are stable for approximately two weeks when stored at room temperature. As the oxidation layer and particles increase, the conductivity and the number and activity of the surface groups of MXenes are significantly affected, thereby reducing their performance in biosensors. In order to address the issue of oxidation, it is possible to enhance the stability of MXenes through surface modification[130,131] or the application of protective coatings.[132,133]

While MXenes exhibit an abundance of surface functional groups that make them biocompatible, the long-term stability and biocompatibility of MXenes in biological systems remain challenges to be addressed. There is a possibility that MXenes may induce cytotoxicity or immune reactions when they come into contact with biological samples. Moreover, some MXene materials with high fluorine contents may have adverse effects on organisms. In the context of long-term applications or implantable devices, the degradation products may also exert adverse effects on biological tissues. Therefore, by optimizing the surface functional groups of MXenes or applying biofriendly coatings on the surface of MXene materials, such as introducing biodegradable functional groups or natural polymers, their stability in biological samples is enhanced and their cell-friendliness is improved. This could further enhance their potential for *in vivo* monitoring and clinical applications.

The development of MXene-based sensor materials has yet to overcome the challenge of recognizing specific biological target molecules. In complex biological samples, the numerous reactive groups on the surface of MXenes can bind nonspecifically to multiple substances simultaneously, thereby affecting the accuracy and stability of the sensor's monitoring. Furthermore, improvements are required in the amplification of the acquired signal and the detection range to achieve efficient detection at ultra-low concentrations. It is thus possible to construct a multifunctional sensor platform by combining MXenes with biomolecular recognition elements or nanomaterials such as antibodies, enzymes, DNA probes, and so forth. This enables the efficient recognition of specific target molecules. The combination of MXenes with biomolecular recognition elements and nanomaterials not only enhances the signal amplification effect but also improves sensitivity and selectivity through synergistic effects.

In practice, the samples detected are often not single samples, and MXene biosensors are often required to analyze complex biological samples. The composition of these samples is often diverse; for example, blood contains mainly water and proteins, while proteins mainly include albumin, globulin and fibrinogen. It also contains electrolyte ions (Na^+, K^+, Ca^{2+}, *etc.*), nutrients (glucose, lipids, amino acids, *etc.*), hormones and enzymes, metabolic wastes and gases. These samples contain a large number of interfering substances (proteins, electrolytes, *etc.*) that can have an effect on the sensor's detection signal, leading to signal attenuation or misinterpretation. The principal avenue for addressing this issue is the construction of intelligent sensor platforms, which can enhance the capacity for signal processing and noise elimination in complex detection samples through the incorporation of intelligent signal processing tools, including machine learning algorithms and artificial intelligence macro models. Furthermore, MXenes can be modified through the introduction of specific functional groups while intertwined with intelligent signal processing tools, thereby enabling them to prioritize the recognition of target molecules and suppress and deal with the effects of other interfering substances. MXenes face limitations in practical applications such as poor stability (easy oxidation), dependence of synthesis on a risky fluorine-based etchant and interlayer stacking, a much higher oxidation rate than that of chemically inert graphene and oxidation-resistant MoS_2, and a costly and risky synthesis process. However, MXenes combine high conductivity (close to graphene and far beyond MoS_2), hydrophilic surfaces, and tunable functional groups, endowing them with higher sensitivity and mechanical flexibility in biosensors. In the future, the stability and process bottlenecks need to be addressed through surface passivation (*e.g.*, Al_2O_3 coating) and green synthesis techniques (*e.g.*, the molten salt method) in order to fully utilize the advantages of their electroconductivity–chemical activity synergy.

MXenes typically require a substantial investment in human resources and material resources to mitigate the risks associated with complex chemical treatment. Large-scale preparation of MXenes remains a research topic, and cost-effective optimization has yet to be achieved. Further research should be directed toward the simplification of the MXene preparation process, the exploration of environmentally-friendly techniques (such as fluorine-free etching and the electrochemical stripping method) and the achievement of industrial mass production, which is a crucial step in the commercialization of MXene biosensors.

6. Conclusion

This review systematically explores the integration of MXenes in biosensor development, covering their unique physical, chemical, and structural properties, synthesis and modification methods, and applications in electrochemical, optical, and wearable portable sensing. Meanwhile, discussions are made based on the MXene materials themselves, the application environment and commercialization, and suggestions are made for the direction of the development of MXene materials as biosensors. MXenes have demonstrated considerable potential in the field of biosensors, reinvigorating areas such as disease diagnosis, environmental monitoring and personal health management. Due to their excellent electrical conductivity, rich surface chemical activity, high specific surface area and excellent mechanical properties, MXenes can serve as sensitive and efficient sensing materials, providing an ideal technology platform for the development of new-generation sensors. Additionally, MXene-based flexible sensors are garnering interest due to their prospective applications in wearable devices, offering novel solutions for personalized medicine and real-time monitoring. Despite the current limitations of MXenes, including stability, functionalization modification, scale-up production and biocompatibility, these issues are being addressed through the advancement of material preparation technology and multidisciplinary cross-research. The potential of MXenes will be further realized through the development of antioxidant MXene derivatives, the optimization of functionalization strategies, the exploration of green preparation methods and the establishment of a standardized evaluation system. The prospective applications of MXenes in the domain of biosensors have the potential to facilitate the advancement of precision medicine and environmental protection while also paving the way for more innovative technological avenues that could enhance the efficiency, cost-effectiveness and human-centric design of sensing technology. With continuous technology iteration and multi-disciplinary synergistic innovation, MXenes are expected to become the core material for the next generation of high-performance biosensors, helping to build a healthier, safer and more sustainable future.

Author contributions

Luming Pan: data curation, methodology, and writing – original draft. Dongtao Zhou: data curation, formal analysis, investigation, and writing – review & editing. Yuzhen Wang: funding acquisition, resources, supervision, and writing – review & editing.

Data availability

No primary research results, software or code have been included and no new data were generated or analysed as part of this review.

Conflicts of interest

The authors confirm that this article's content has no conflicts of interest.

Acknowledgements

This work was supported by the National Natural Science Foundation of China (No. 22377055).

References

1 C. Lino, S. Barrias, R. Chaves, F. Adega, P. Martins-Lopes and J. R. Fernandes, *Biochim. Biophys. Acta, Rev. Cancer*, 2022, **1877**, 188726.
2 M. Shoaib, H. Li, I. M. Khan, M. M. Hassan, M. Zareef, S. Niazi and Q. Chen, *Trends Food Sci. Technol.*, 2024, **151**, 104635.
3 A. Williams, M. R. Aguilar, K. G. G. P. Arachchillage, S. Chandra, S. Rangan, S. G. Gupta and J. M. A Vivancos, *ACS Sustainable Chem. Eng.*, 2024, **12**, 10296–10312.
4 Z. Song, S. Zhou, Y. Qin, X. Xia, Y. Sun, G. Han, T. Shu, L. Hu and Q. Zhang, *Biosensors*, 2023, **13**, 630.
5 Q. Wang, C. Jiao, W. Chen, L. Li, X. Zhang, Z. Guo, L. Hu and Y. Fan, *Biosens. Bioelectron.*, 2025, **268**, 116858.
6 M. Almalaysha, A. Singh, S. A. Muhsin, A. V. Carlson, K. E. Trout, A. Morey, S. Zhang, L. H. Channaiah and M. Almasri, *Sens. Actuators Rep.*, 2025, **9**, 100257.
7 E. Proniewicz, *Spectrochim. Acta, Part A*, 2023, **288**, 122207.
8 Y. A. Sihombing, Uperianti, R. I. Sari, B. R. Hermanto, M. Handayani, S. P. Kusumocahyo, M. F. Ulum, R. Siburian, C. Kurniawan, N. Widiarti, Y. W. Hartati and I. Anshori, *Sens. Actuators Rep.*, 2024, **8**, 100223.
9 A. N. Herdina, A. Bozdogan, P. Aspermair, J. Dostalek, M. Klausberger, N. Lingg, M. Cserjan-Puschmann, P. P. Aguilar, S. Auer, H. Demirtas, J. Andersson, F. Lötsch, B. Holzer, A. Steinrigl, F. Thalhammer, J. Schellnegger, M. Breuer, W. Knoll and R. Strassl, *Biosens. Bioelectron.*, 2025, **267**, 116807.
10 M. Naguib, M. W. Barsoum and Y. Gogotsi, *Adv. Mater.*, 2021, **33**, e2103393.
11 M. Naguib, M. Kurtoglu, V. Presser, J. Lu, J. Niu, M. Heon, L. Hultman, Y. Gogotsi and M. W. Barsoum, *Adv. Mater.*, 2011, **23**, 4248–4253.
12 A. Hermawan, T. Amrillah, A. Riapanitra, W.-J. Ong and S. Yin, *Adv. Healthcare Mater.*, 2021, **10**, 2100970.
13 M. Liao, Z. Zheng, H. Jiang, M. Ma, L. Wang, Y. Wang and S. Zhuang, *Sci. Total Environ.*, 2024, **912**, 169014.
14 L. Li, J. Pan, L. Chang, Z. Liu, G. Wu and Y. Hu, *Chem. Eng. J.*, 2024, **482**, 148988.
15 W. Eom, H. Shin, R. B. Ambade, S. H. Lee, K. H. Lee, D. J. Kang and T. H. Han, *Nat. Commun.*, 2020, **11**, 2825.
16 Z. Otgonbayar and W.-C. Oh, *FlatChem*, 2023, **40**, 100524.

17 D. Saha, J. Dalmieda and V. Patel, *ACS Appl. Electron. Mater.*, 2023, **5**, 2933–2955.
18 X. Mao, L. Qian, L. Tian, X. Chen, W. Wu and Z. Li, *Nano Lett.*, 2024, **24**, 15151–15158.
19 T. R. Dmytriv and V. I. Lushchak, *Chem. Rec.*, 2024, **24**, e202300338.
20 E. Morales-Narváez, L. Baptista-Pires, A. Zamora-Gálvez and A. Merkoçi, *Adv. Mater.*, 2017, **29**, 1604905.
21 A. T. Lawal, *Biosens. Bioelectron.*, 2018, **106**, 149–178.
22 D.-Y. Zhang, H. Liu, M. R. Younis, S. Lei, Y. Chen, P. Huang and J. Lin, *J. Nanobiotechnol.*, 2022, **20**, 53.
23 Y. Ding, S. Zhang, X. Zang, M. Ding and C. Ding, *Microchim. Acta*, 2023, **191**, 5.
24 S. K. Nemani, B. Zhang, B. C. Wyatt, Z. D. Hood, S. Manna, R. Khaledialidusti, W. Hong, M. G. Sternberg, S. K. R. S. Sankaranarayanan and B. Anasori, *ACS Nano*, 2021, **15**, 12815–12825.
25 X. Zhang, Z. Ni, X. Bai, H. Shen, Z. Wang, C. Wei, K. Tian, B. Xi, S. Xiong and J. Feng, *Adv. Energy Mater.*, 2023, **13**, 2301349.
26 U. Khan, Y. Luo, L. B. Kong and W. Que, *J. Alloys Compd.*, 2022, **926**, 166903.
27 P. Urbankowski, B. Anasori, T. Makaryan, D. Er, S. Kota, P. L. Walsh, M. Zhao, V. B. Shenoy, M. W. Barsoum and Y. Gogotsi, *Nanoscale*, 2016, **8**, 11385–11391.
28 S. Wang, Y. Liu, Y. Liu and W. Hu, *Chem. Eng. J.*, 2023, **452**, 139512.
29 M. Ghidiu, M. R. Lukatskaya, M.-Q. Zhao, Y. Gogotsi and M. W. Barsoum, *Nature*, 2014, **516**, 78–81.
30 M. Alhabeb, K. Maleski, B. Anasori, P. Lelyukh, L. Clark, S. Sin and Y. Gogotsi, *Chem. Mater.*, 2017, **29**, 7633–7644.
31 T. Bai, W. Wang, G. Xue, S. Li, W. Guo, M. Ye and C. Wu, *ACS Appl. Mater. Interfaces*, 2021, **13**, 57576–57587.
32 K. Arole, J. W. Blivin, A. M. Bruce, S. Athavale, I. J. Echols, H. Cao, Z. Tan, M. Radovic, J. L. Lutkenhaus and M. J. Green, *Chem. Commun.*, 2022, **58**, 10202–10205.
33 P. Urbankowski, B. Anasori, K. Hantanasirisakul, L. Yang, L. Zhang, B. Haines, S. J. May, S. J. L. Billinge and Y. Gogotsi, *Nanoscale*, 2017, **9**, 17722–17730.
34 Y. Guo, Q. Zhu, Z. Wang, Y. Ye, J. Hu, J. Shang, B. Li, Z. Du and S. Yang, *Adv. Energy Mater.*, 2024, **14**, 2304149.
35 J. Zhu, S. Zhu, Z. Cui, Z. Li, S. Wu, W. Xu, T. Ba, Y. Liang and H. Jiang, *Energy Storage Mater.*, 2024, **70**, 103503.
36 W. Sun, S. A. Shah, Y. Chen, Z. Tan, H. Gao, T. Habib, M. Radovic and M. J. Green, *J. Mater. Chem. A*, 2017, **5**, 21663–21668.
37 L. Liu, H. Zschiesche, M. Antonietti, M. Gibilaro, P. Chamelot, L. Massot, P. Rozier, P.-L. Taberna and P. Simon, *Adv. Energy Mater.*, 2023, **13**, 2203805.
38 K. C. Chan, X. Guan, T. Zhang, K. Lin, Y. Huang, L. Lei, Y. Georgantas, Y. Gogotsi, M. A. Bissett and I. A. Kinloch, *J. Mater. Chem. A*, 2024, **12**, 25165–25175.
39 K. P. Divya, S. Keerthana, C. Viswanathan and N. Ponpandian, *Microchim. Acta*, 2023, **190**, 116.
40 H. Wang, H. Li, Y. Huang, M. Xiong, F. Wang and C. Li, *Biosens. Bioelectron.*, 2019, **142**, 111531.
41 S. Kumar, Y. Lei, N. H. Alshareef, M. A. Quevedo-Lopez and K. N. Salama, *Biosens. Bioelectron.*, 2018, **121**, 243–249.
42 X. Jiang, J. Ma, K. Xue, J. Chen, Y. Zhang, G. Zhang, K. Wang, Z. Yao, Q. Hu, C. Lin, B. Lei and C. Mao, *ACS Nano*, 2024, **18**, 4269–4286.
43 H. Niu, S. Cai, X. Liu, X. Huang, J. Chen, S. Wang and S. Zhang, *Anal. Methods*, 2022, **14**, 843–849.
44 Y. Zheng, Y. Zhou, X. Cui, H. Yin and S. Ai, *Mater. Today Chem.*, 2022, **24**, 100878.
45 M. Lian, Y. Shi, W. Zhang, J. Zhao and D. Chen, *J. Electroanal. Chem.*, 2022, **904**, 115849.
46 L. You, Z. Zheng, W. Xu, Y. Wang, W. Xiong, C. Xiong and S. Wang, *Int. J. Biol. Macromol.*, 2024, **263**, 130439.
47 K. S. Rizi, B. Hatamluyi, M. Darroudi, Z. Meshkat, E. Aryan, S. Soleimanpour and M. Rezayi, *Microchem. J.*, 2022, **179**, 107467.
48 B. Singh, R. Bahadur, M. Gandhi and R. Srivastava, *Polym. Bull.*, 2023, **80**, 11329–11342.
49 W. Y. Chen, C. D. Sullivan, S.-N. Lai, C.-C. Yen, X. Jiang, D. Peroulis and L. A. Stanciu, *ACS Omega*, 2022, **7**, 29195–29203.
50 C. Zhang, B. Anasori, A. Seral-Ascaso, S.-H. Park, N. McEvoy, A. Shmeliov, G. S. Duesberg, J. N. Coleman, Y. Gogotsi and V. Nicolosi, *Adv. Mater.*, 2017, **29**, 1702678.
51 X. Wang, X. Yuan, D. Wang, W. Dong, C. Dong, Y. Zhang, T. Lin and F. Huang, *ACS Appl. Energy Mater.*, 2018, **1**, 876–882.
52 M. Cao, D.-B. Xiong, L. Yang, S. Li, Y. Xie, Q. Guo, Z. Li, H. Adams, J. Gu, T. Fan, X. Zhang and D. Zhang, *Adv. Funct. Mater.*, 2019, **29**, 1806792.
53 D.-B. Xiong, M. Cao, Q. Guo, Z. Tan, G. Fan, Z. Li and D. Zhang, *ACS Nano*, 2015, **9**, 6934–6943.
54 J. Hwang, T. Yoon, S. H. Jin, J. Lee, T.-S. Kim, S. H. Hong and S. Jeon, *Adv. Mater.*, 2013, **25**, 6724–6729.
55 Y. Chen, X. Zhang, E. Liu, C. He, C. Shi, J. Li, P. Nash and N. Zhao, *Sci. Rep.*, 2016, **6**, 19363.
56 N. H. Solangi, R. R. Karri, N. M. Mubarak, S. A. Mazari and B. P. Sharma, *Nanoscale*, 2024, **16**, 21216–21263.
57 S. Chen, D. Zheng, Q. Cen, C. G. Yoo, L. Zhong, D. Yang and X. Qiu, *Small*, 2024, **20**, 2400603.
58 M. Zhang, F. Héraly, M. Yi and J. Yuan, *Cell Rep. Phys. Sci.*, 2021, **2**, 100449.
59 N. Bandaru, C. V. Reddy, K. Vallabhudasu, M. Vijayalakshmi, K. R. Reddy, B. Cheolho, J. Shim and T. M. Aminabhavi, *Chem. Eng. J.*, 2024, **500**, 157317.
60 Z. Gong, Q. Jiang, W. Bai, P. Wang, M. Gao, D. Cao, M. Zhou, Y. Sun and K. Zhu, *J. Energy Storage*, 2024, **88**, 111545.
61 Y. Jin, J. Geng, Y. Wang, Z. Zhao, Z. Chen, Z. Guo, L. Pei, F. Ren, Z. Sun and P.-G. Ren, *Surf. Interfaces*, 2024, **53**, 104999.
62 D. Tyndall, L. Gannon, L. Hughes, J. Carolan, S. Pinilla, S. Jaśkaniec, D. Spurling, O. Ronan, C. McGuinness, N. McEvoy, V. Nicolosi and M. P. Browne, *npj 2D Mater. Appl.*, 2023, **7**, 15.

63 J. Ding, B. Xin, J. Li, H. Deng, Q. Yuan, S. Liu and Q. Chen, *ACS Appl. Nano Mater.*, 2024, **7**, 24123–24131.
64 I. Raheem, N. M. Mubarak, R. R. Karri, N. H. Solangi, A. S. Jatoi, S. A. Mazari, M. Khalid, Y. H. Tan, J. R. Koduru and G. Malafaia, *Chemosphere*, 2023, **311**, 137056.
65 W. Liu, Z. Chen, Z. Ma, J. Li, Y. Liu, Y. Zhang and Y. Feng, *Chem. Eng. J.*, 2024, **494**, 153149.
66 X. Bai and J. Guan, *Small Struct.*, 2023, **4**, 2200354.
67 K. Zhang, D. Li, H. Cao, Q. Zhu, C. Trapalis, P. Zhu, X. Gao and C. Wang, *Chem. Eng. J.*, 2021, **424**, 130340.
68 D. Li, H. Liang and Y. Zhang, *Carbon*, 2024, **226**, 119205.
69 B. Yamunasree, S. Kim, Y. H. Park, J. K. R. Modigunta, J. Kim, A. K. Astakala, S. J. Lee, G. Murali, W. Lee and I. In, *Carbon*, 2024, **228**, 119364.
70 S. Ajith, F. Almomani and H. Qiblawey, *J. Environ. Chem. Eng.*, 2024, **12**, 112078.
71 C. Chen, B. Wang, J. Xu, L. Fei, S. Raza, B. Li, Q. Zeng, L. Shen and H. Lin, *Small*, 2024, **20**, 2311427.
72 S. Wan, X. Li, Y. Chen, N. Liu, Y. Du, S. Dou, L. Jiang and Q. Cheng, *Science*, 2021, **374**, 96–99.
73 Y. Cheng, Y. Xie, H. Cao, L. Li, Z. Liu, S. Yan, Y. Ma, W. Liu, Y. Yue, J. Wang, Y. Gao and L. Li, *Chem. Eng. J.*, 2023, **453**, 139823.
74 L.-X. Liu, W. Chen, H.-B. Zhang, L. Ye, Z. Wang, Y. Zhang, P. Min and Z.-Z. Yu, *Nano-Micro Lett.*, 2022, **14**, 111.
75 Y. Zhang, K. Chen, Y. Li, J. Lan, B. Yan, L. Shi and R. Ran, *ACS Appl. Mater. Interfaces*, 2019, **11**, 47350–47357.
76 Y. Zhou, Y. Zou, Z. Peng, C. Yu and W. Zhong, *Nanoscale*, 2020, **12**, 20797–20810.
77 Z. Xiao, Z. Li, X. Meng and R. Wang, *J. Mater. Chem. A*, 2019, **7**, 22730–22743.
78 Y. Cai, Z. Yu, L. Cheng, Y. Yuan, S. Ren, Y. Chai, M. Chen, X. Huang and Y. Li, *J. Mater. Chem. C*, 2024, **12**, 11846–11860.
79 B. Li, N. Wu, Y. Yang, F. Pan, C. Wang, G. Wang, L. Xiao, W. Liu, J. Liu and Z. Zeng, *Adv. Funct. Mater.*, 2023, **33**, 2213357.
80 W. Liu, M. Li, X. Feng, S. Gong, K. Yu and Z. Zhu, *Chem. Eng. J.*, 2024, **496**, 154247.
81 W. Liu, D. Luo, M. Zhang, J. Chen, M. Li, A. Chen, S. Xi and A. Yu, *Nano Energy*, 2024, **122**, 109332.
82 S. Panda, K. Deshmukh, S. K. K. Pasha, J. Theerthagiri, S. Manickam and M. Y. Choi, *Coord. Chem. Rev.*, 2022, **462**, 214518.
83 F. Ming, H. Liang, G. Huang, Z. Bayhan and H. N. Alshareef, *Adv. Mater.*, 2021, **33**, 2004039.
84 Y. Li, X. Feng, W. Y. Lieu, L. Fu, C. Zhang, T. Ghosh, A. Thakur, B. C. Wyatt, B. Anasori, W. Liu, Q. Zhang, J. Lu and Z. W. Seh, *Adv. Funct. Mater.*, 2023, **33**, 2303067.
85 H. Liu, Z. Xin, B. Cao, B. Zhang, H. J. Fan and S. Guo, *Adv. Sci.*, 2024, **11**, 2305806.
86 N. Zare, H. Karimi-Maleh, Z. Zhang, Y. Wen, N. Zhong and L. Fu, *Adv. Compos. Hybrid Mater.*, 2024, **7**, 165.
87 S. C. G, L. Gokavi, C. H. Ravikumar and R. G. Balarkishna, *Biosens. Bioelectron.*, 2025, **271**, 117028.
88 B. Ding, Z. Zhu, C. Guo, J. Li, Y. Gan and M. Yu, *Acta Pharm. Sin. B*, 2024, **14**, 2006–2025.
89 X. Bian, D. Yang, Y. Zeng, T. Yang, Q. Xia and T. Hu, *Sens. Actuators Rep.*, 2024, **8**, 100232.
90 M. Gupta, A. Verma, P. Chaudhary and B. C. Yadav, *Mater. Adv.*, 2023, **4**, 3989–4010.
91 A. Rudie, A. M. Schornack, Q. Wu, Q. Zhang and D. Wang, *Biosensors*, 2022, **12**, 332.
92 S. Siraj, G. Bansal, B. Hasita, S. Srungaram, S. K. S, F. J. Rybicki, S. Sonkusale and P. Sahatiya, *ACS Appl. Nano Mater.*, 2024, **7**, 11350–11361.
93 A. Dhillon, N. Singh, M. Nair and D. Kumar, *Chemosphere*, 2022, **303**, 135166.
94 G. Manasa and C. S. Rout, *Mater. Adv.*, 2024, **5**, 83–122.
95 L. Guo, J. Wang, H. Han, P. Wang, Y. Lu, Q. Yuan, C. Du, S. Yin, Y. Zhou and C. Zhang, *ACS Appl. Mater. Interfaces*, 2024, **16**, 62421–62428.
96 M. Zahoor, M. Ikram, S. Khan and S. Ali, *Inorg. Chem. Commun.*, 2024, **170**, 113157.
97 L. Wen, J. Dong, H. Yang, J. Zhao, Z. Hu, H. Han, C. Hou, X. Luo and D. Huo, *Sci. Total Environ.*, 2022, **851**, 158325.
98 E. Cheraghipour and M. Pakshir, *Chemosphere*, 2020, **260**, 127560.
99 K. Ji, Z. Liang, P. Wang, Z. Li, Q. Ma and X. Su, *Chem. Eng. J.*, 2024, **495**, 153598.
100 D. George, C. H. Ravikumar, J. J. Philip and R. G. Balakrishna, *J. Mater. Chem. C*, 2024, **12**, 18345–18355.
101 T. A. Oyehan, S. A. Ganiyu, C. Pfrang, M. Walker and E. Valsami-Jones, *Chem. Eng. J.*, 2024, **492**, 152217.
102 Q. Wang, Y. Xiong, J. Xu, F. Dong and Y. Xiong, *Sep. Purif. Technol.*, 2022, **286**, 120506.
103 W. Y. Chen, S.-N. Lai, C.-C. Yen, X. Jiang, D. Peroulis and L. A. Stanciu, *ACS Nano*, 2020, **14**, 11490–11501.
104 X. Ming, A. Guo, Q. Zhang, Z. Guo, F. Yu, B. Hou, Y. Wang, K. P. Homewood and X. Wang, *Carbon*, 2020, **167**, 285–295.
105 Y. G. Song, Y.-S. Shim, J. M. Suh, M.-S. Noh, G. S. Kim, K. S. Choi, B. Jeong, S. Kim, H. W. Jang, B.-K. Ju and C.-Y. Kang, *Small*, 2019, **15**, 1970214.
106 J. Ding, Q. Wang, X. Liu, S. Li and H. Li, *J. Hazard. Mater.*, 2024, **480**, 136261.
107 V. T. Le, Y. Vasseghian, V. D. Doan, T. T. T. Nguyen, T.-T. Thi Vo, H. H. Do, K. B. Vu, Q. H. Vu, T. Dai Lam and V. A. Tran, *Chemosphere*, 2022, **291**, 133025.
108 N. M. Tran, Q. T. H. Ta and J.-S. Noh, *Mater. Chem. Phys.*, 2021, **273**, 125087.
109 S. Zhu, W. Yang, C. Hao, Z. Xu, H. Tao, X. Tang and Y. Wang, *Small*, 2025, **21**, 2405644.
110 Z. Wang, F. Zhou, Y. Li, S. Wang, W. Li, H. Liu, M. Hu, F. Wang, L. Wang and J. Mao, *Chem. Eng. J.*, 2024, **498**, 155352.
111 C. Zhang, P.-a. Zong, Z. Ge, Y. Ge, J. Zhang, Y. Rao, Z. Liu and W. Huang, *Nano Energy*, 2023, **118**, 109037.
112 R. D. Nagarajan, A. Sundaramurthy and A. K. Sundramoorthy, *Chemosphere*, 2022, **286**, 131478.

113 K. Zhang, Z. Fan, Y. Huang, Y. Ding and M. Xie, *Talanta*, 2022, **236**, 122868.
114 C. Wen, B. Zhao, Y. Liu, C. Xu, Y. Wu, Y. Cheng, J. Liu, Y. Liu, Y. Yang, H. Pan, J. Zhang, L. Wu and R. Che, *Adv. Funct. Mater.*, 2023, **33**, 2214223.
115 H. Lin, X. Wang, L. Yu, Y. Chen and J. Shi, *Nano Lett.*, 2017, **17**, 384–391.
116 T. Xu, S. Tan, S. Li, T. Chen, Y. Wu, Y. Hao, C. Liu and G. Ji, *Adv. Funct. Mater.*, 2024, **34**, 2400424.
117 R. Kumar, S. Pal and Y. K. Prajapati, *Plasmonics*, 2023, **18**, 1787–1798.
118 X. Dai, C. Song, C. Qiu, L. Wu and Y. Xiang, *IEEE Sens. J.*, 2019, **19**, 11834–11838.
119 M. Hu, T. Hu, Z. Li, Y. Yang, R. Cheng, J. Yang, C. Cui and X. Wang, *ACS Nano*, 2018, **12**, 3578–3586.
120 R. K. Choudhury, B. R. Bhagat, K. H. Mali, R. Pokar and A. Dashora, *Appl. Surf. Sci.*, 2022, **603**, 154426.
121 Y. Sun, Y. Du, Y. Zhang, J. Yang, J. Liu, R. Tian, J. Wang, Q. Li, X. He and J. Fu, *J. Mater. Chem. A*, 2024, **12**, 22166–22179.
122 Y. Wang, S. Wang, N. Dong, W. Kang, K. Li and Z. Nie, *Anal. Chem.*, 2020, **92**, 4623–4629.
123 H. Li, Y. Wen, X. Zhu, J. Wang, L. Zhang and B. Sun, *ACS Sustainable Chem. Eng.*, 2020, **8**, 520–526.
124 Q. Lu, J. Wang, B. Li, C. Weng, X. Li, W. Yang, X. Yan, J. Hong, W. Zhu and X. Zhou, *Anal. Chem.*, 2020, **92**, 7770–7777.
125 X. Chen, X. Sun, W. Xu, G. Pan, D. Zhou, J. Zhu, H. Wang, X. Bai, B. Dong and H. Song, *Nanoscale*, 2018, **10**, 1111–1118.
126 L. Lu, X. Han, J. Lin, Y. Zhang, M. Qiu, Y. Chen, M. Li and D. Tang, *Analyst*, 2021, **146**, 2664–2669.
127 L. Li, Y. Chen and J.-J. Zhu, *Anal. Chem.*, 2017, **89**, 358–371.
128 H. Zhang, Z. Wang, Q. Zhang, F. Wang and Y. Liu, *Biosens. Bioelectron.*, 2019, **124–125**, 184–190.
129 Y. Sun, P. Li, Y. Zhu, X. Zhu, Y. Zhang, M. Liu and Y. Liu, *Biosens. Bioelectron.*, 2021, **194**, 113600.
130 W. Eom, H. Shin, W. Jeong, R. B. Ambade, H. Lee and T. H. Han, *Mater. Horiz.*, 2023, **10**, 4892–4902.
131 A. Chae, G. Murali, S.-Y. Lee, J. Gwak, S. J. Kim, Y. J. Jeong, H. Kang, S. Park, A. S. Lee, D.-Y. Koh, I. In and S.-J. Park, *Adv. Funct. Mater.*, 2023, **33**, 2213382.
132 W. Qian, Y. Si, P. Chen, C. Tian, Z. Wang, P. Li, S. Li and D. He, *Small*, 2024, **20**, 2403149.
133 C. Yang, J. Hu, L. Liu, S. Wu, M. Pan, Y. Liu, H. Wang, P. Li, Q. Zhang, W. Qiu and H. Luo, *Microsyst. Nanoeng.*, 2024, **10**, 41.